

Analysis of continuous-time Markovian -SIS epidemics on networks

Achterberg, Massimo A.; Prasse, Bastian; Van Mieghem, Piet

DOI

[10.1103/PhysRevE.105.054305](https://doi.org/10.1103/PhysRevE.105.054305)

Publication date

2022

Document Version

Final published version

Published in

Physical Review E

Citation (APA)

Achterberg, M. A., Prasse, B., & Van Mieghem, P. (2022). Analysis of continuous-time Markovian -SIS epidemics on networks. *Physical Review E*, 105(5), Article 054305. <https://doi.org/10.1103/PhysRevE.105.054305>

Important note

To cite this publication, please use the final published version (if applicable). Please check the document version above.

Copyright

Other than for strictly personal use, it is not permitted to download, forward or distribute the text or part of it, without the consent of the author(s) and/or copyright holder(s), unless the work is under an open content license such as Creative Commons.

Takedown policy





Please contact us and provide details if you believe this document breaches copyrights. We will remove access to the work immediately and investigate your claim.

Green Open Access added to TU Delft Institutional Repository

'You share, we take care!' - Taverne project

<https://www.openaccess.nl/en/you-share-we-take-care>

Otherwise as indicated in the copyright section: the publisher is the copyright holder of this work and the author uses the Dutch legislation to make this work public.

Analysis of continuous-time Markovian ε -SIS epidemics on networksMassimo A. Achterberg ^{*}, Bastian Prasse , and Piet Van Mieghem *Faculty of Electrical Engineering, Mathematics and Computer Science, Delft University of Technology, P.O. Box 5031, 2600 GA Delft, The Netherlands* (Received 28 October 2021; accepted 19 April 2022; published 9 May 2022)

We analyze continuous-time Markovian ε -SIS epidemics with self-infections on the complete graph. The majority of the graphs are analytically intractable, but many physical features of the ε -SIS process observed in the complete graph can occur in any other graph. In this work, we illustrate that the timescales of the ε -SIS process are related to the eigenvalues of the tridiagonal matrix of the SIS Markov chain. We provide a detailed analysis of all eigenvalues and illustrate that the eigenvalues show staircases, which are caused by the nearly degenerate (but strictly distinct) pairs of eigenvalues. We also illustrate that the ratio between the second-largest and third-largest eigenvalue is a good indicator of metastability in the ε -SIS process. Additionally, we show that the epidemic threshold of the Markovian ε -SIS process can be accurately approximated by the effective infection rate for which the third-largest eigenvalue of the transition matrix is the smallest. Finally, we derive the exact mean-field solution for the ε -SIS process on the complete graph, and we show that the mean-field approximation does not correctly represent the metastable behavior of Markovian ε -SIS epidemics.

DOI: [10.1103/PhysRevE.105.054305](https://doi.org/10.1103/PhysRevE.105.054305)**I. INTRODUCTION**

Over the past 100 years, many epidemic diseases have plagued humanity. Most epidemic outbreaks tend to emerge quickly, but they take much longer to disappear [1]. One of the main reasons is reinfections. A common example of a disease with reinfections is influenza, which affects large portions of the population during the winter season. The influenza virus strain keeps mutating slightly, thereby bypassing the human immune system while maintaining most of its viral properties. Another example of recurring diseases are sexually transmitted diseases, such as chlamydia and gonorrhoea. Contrary to influenza, sexually transmitted diseases do not mutate, but people can simply be reinfected after recovering from the disease.

Initially, epidemic outbreaks spread exponentially fast, because most individuals in the population are susceptible to the new disease, as happened with the COVID-19 pandemic. In a closed and well-mixed population, the number of infected individuals stabilizes after a short time and continues to oscillate around the *prevalence*, which is defined as the average number of infected individuals. Then, the epidemic process is in the *metastable* or *quasistationary state*, because the number of infected individuals remains in the vicinity of the prevalence for a long period of time, whereafter the process eventually converges to its steady state. The steady state of most epidemic processes is the overall-healthy state, which corresponds to the situation in which the disease has disappeared completely from the population.

One of the simplest stochastic epidemic models with reinfections is the continuous-time Markovian susceptible-infected-susceptible (SIS) model, in which individuals are

either infectious (I) or healthy, but susceptible (S). The contact graph G represents the N individuals as nodes and specifies the L contacts between all pairs of individuals as links. The Markovian SIS dynamics consists of two independent Poisson processes: (i) the infected nodes can cure with rate δ , and (ii) infected nodes can infect their connected, susceptible neighbors with rate β . The curing process is a nodal process, whereas the infection process evolves over the links between pairs of nodes. Occasionally, a third, independent self-infection process with self-infection rate ε is considered, which describes background or indirect infections. Infections may happen either through direct contact or indirectly, for example after touching infected surfaces or inhaling air in a closed room previously contaminated by an infected individual. The Markovian ε -SIS model consists of three independent Poisson processes: (i) the curing process with rate δ , (ii) infection process with rate β , and (iii) self-infection process with rate ε . Given that the ε -SIS model consists of independent Poisson processes, we can describe the time-dependent behavior of the ε -SIS model as a continuous-time Markov chain with 2^N states. However, continuous-time Markovian modeling implies that the infection and curing times are exponentially distributed. Measurements in real epidemics seem to suggest that the infection time follows a bell-shaped distribution (such as Gamma, Weibull, or log-normal distributions [2,3]). This requires non-Markovian analysis, which is, unfortunately, considerably more complex (see, e.g., [4]) and is currently insufficiently developed to compute time-dependent infection probabilities.

The continuous-time Markovian SIS process without self-infections on static networks has been investigated thoroughly [5]. Even on the complete graph, quantifying the average time spent in the metastable state appears challenging [6]. The major issue is that the metastable state is not stable; it collapses eventually due to a rare occurrence of successive

^{*}M.A.Achterberg@tudelft.nl

curing to the absorbing or overall-healthy state [7]. Several approaches have been proposed to quantify the metastable state in the Markovian SIS model. Jacquez and Simon [8] introduced an epidemic process that prevents the original SIS process from entering the absorbing state at time t . Their reduced SIS model has a unique steady state, which can be related to the metastable state of the original SIS model. Cator and Van Mieghem [9] constructed a similar modified process: If only a single node is infected, then the modified process forbids the curing of that node. Effectively, their modified SIS process is equivalent to the SIS process, with the exception that the transitions to the absorbing state have been removed. De Oliveira and Dickman [10] proposed to store the complete time lapse of the SIS model. Once the process converges to the absorbing state, the process jumps to a randomly selected sample from the history of the SIS process. Keeling and Ross [11] and Hill *et al.* [12] introduced a self-infection process ε on the complete graph. In addition to the usual infection and curing processes, the nodes in the modified process can be infected by external sources, which are modeled as self-infections. Van Mieghem and Cator [13] generalized the ε -SIS model from the complete graph to general networks. Introducing a small amount of self-infections removes the absorbing state, reestablishes an irreducible Markov chain with a well-defined steady state different from the overall-healthy state and allows for a comparison between the ε -SIS model and the SIS model without self-infections. Finally, the 2^N -state Markov chain, described by 2^N linear differential equations, is often approximated by a mean-field approximation with N nonlinear differential equations. The simplest mean-field approximation for the SIS model on networks is called the N-Intertwined mean-field approximation (NIMFA), and it assumes that the infection state of any two nodes is uncorrelated [14–17]. A mean-field approximation is generally an adequate approximation for large, dense graphs with homogeneous transition rates and for infection rates sufficiently larger than the epidemic threshold. The accuracy of NIMFA with respect to the Markovian SIS process is studied in [18] for various graph types. A key difference is the possibility of die-outs in the stochastic model, albeit with a very small probability, whereas the mean-field model either converges to the endemic equilibrium or to the all-healthy state, and excludes the possibility of sudden die-outs.

The continuous-time Markovian ε -SIS process on the complete graph can be described by a birth and death process (BDP). BDPs can be solved by computing the probability generating function and solving the corresponding partial differential equation [19,20]. Unfortunately, solving the partial differential equation seems infeasible for ε -SIS dynamics (see Ref. [21], Appendix A). Alternatively, one may compute the Rayleigh-Ritz coefficient of the partial differential equations to derive bounds for the eigenvalues. There are also several approaches to compute the eigenvalues of BDPs exactly. One possibility is to consider the orthogonal polynomials that correspond to the BDPs, which are the Tricomi-Carlitz polynomials. The zeros of the Tricomi-Carlitz polynomials correspond to the eigenvalues of the BDP. Unfortunately, not many results are known for the zeros of the Tricomi-Carlitz polynomials [22]. Alternatively, one may

solve for the eigenvalues directly, resulting in a continued fraction expansion [23], or one can also derive bounds on the eigenvalues, e.g., by the Cauchy interlacing theorem or using a Fokker-Planck approximation [24].

The eigenvalues of Markov chains and their relation to metastability have been studied in several works. Artajelo [25] studied the second-largest eigenvalue in general Markov chains in both continuous time and discrete time. Holme and Tupikina [26] computed the exact second-largest eigenvalue in SIS epidemics for all nonisomorphic graphs with $3 \leq N \leq 8$ nodes. For an arbitrary graph size N , exact results of the ε -SIS model can be obtained only for a few graphs, such as the complete graph and the star graph [9]. For the complete graph with homogeneous transition rates and no self-infections, several analytical results have been obtained, such as the average time before extinction [24,27–29] and the average time between the onset of the disease and the arrival at the metastable state [30,31].

In this work, we study continuous-time Markovian ε -SIS epidemics on the complete graph from an eigenvalue perspective by computing *all* its eigenvalues. Although we realize that the complete graph is far from a realistic setting, we derive many qualitative properties of the ε -SIS process which, we believe, may also hold for other graphs. We describe the continuous-time Markov chain for the complete graph in Sec. II. We additionally derive the general solution of the Markov chain. We introduce the concept of metastability in Sec. III, and we derive the exact mean-field solution in Sec. IV. We return to the Markovian ε -SIS process in Sec. V and provide a detailed analysis of all eigenvalues. We numerically identify the influence of the infection rate β , self-infection rate ε , and network size N on the eigenvalues in Sec. VI. Finally, we present conclusions in Sec. VII.

II. THE ε -SIS PROCESS ON THE COMPLETE GRAPH

The Markov chain of the ε -SIS process on the complete graph can be described as follows. In the Markov chain \mathcal{M} , each state M denotes the number of infected individuals in the population. Since the population consists of N individuals, the number M of infected nodes ranges from zero to N . Thus, the Markov chain \mathcal{M} has $N + 1$ states with the transition rates (derived in Ref. [32], p. 474)

$$\begin{aligned} M &\mapsto M + 1 && \text{at rate } (\beta M + \varepsilon)(N - M), \\ M &\mapsto M - 1 && \text{at rate } \delta M, \end{aligned}$$

where β denotes the infection rate, δ is the curing rate, and ε is the self-infection rate in the complete graph K_N . The Markov chain \mathcal{M} is a birth and death process with birth rate $\lambda_k = (\beta k + \varepsilon)(N - k)$ that is quadratic in k , and death rate $\mu_k = \delta k$ that is linear in k and is drawn in Fig. 1.

We compute the probability that k nodes are infected at time t in the Markov chain \mathcal{M} . Let $M(t)$ be the number of infected nodes at time t . By introducing $s_k(t) = \Pr[M(t) = k]$ as the probability that the number $M(t)$ of infected nodes at time t equals k , the following differential equations describe

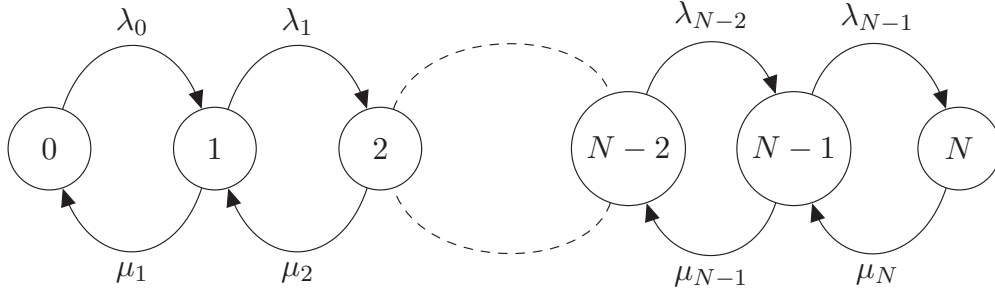


FIG. 1. The Markov chain \mathcal{M} of the ε -SIS process on the complete graph is a finite birth and death process with birth rate $\lambda_k = (\beta k + \varepsilon)(N - k)$ and death rate $\mu_k = \delta k$. The state $M = 0, \dots, N$ of the Markov chain denotes the number of infected nodes in the graph. Furthermore, β is the infection rate, δ is the curing rate, and ε is the self-infection rate.

the exact dynamics of the Markov chain \mathcal{M} :

$$\begin{aligned} \frac{ds_0}{dt} &= \mu_1 s_1(t) - \lambda_0 s_0(t), \\ \frac{ds_k}{dt} &= -(\lambda_k + \mu_k) s_k(t) + \lambda_{k-1} s_{k-1}(t) + \mu_{k+1} s_{k+1}(t), \\ &k = 1, \dots, N-1, \\ \frac{ds_N}{dt} &= \lambda_{N-1} s_{N-1}(t) - \mu_N s_N(t), \end{aligned}$$

If the curing rate $\delta > 0$, the ε -SIS process can be simplified by introducing the rescaled time $\tilde{t} = \delta t$. We additionally

define the scaled birth rate $\tilde{\lambda}_k = \lambda_k / \delta = (\tau k + \varepsilon^*)(N - k)$ and the scaled death rate $\tilde{\mu}_k = \mu_k / \delta = k$, where the effective infection rate $\tau = \beta / \delta$ and the effective self-infection rate $\varepsilon^* = \varepsilon / \delta$. We emphasize that the scaled time \tilde{t} , the effective infection rate τ , and the effective self-infection rate ε^* are dimensionless variables. Introducing the $(N + 1) \times 1$ vector $\mathbf{s} = (s_0, \dots, s_N)^T$, the linear differential equations can be written in matrix notation:

$$\frac{d\mathbf{s}^T}{d\tilde{t}} = \mathbf{s}^T P, \quad (1)$$

where P is the $(N + 1) \times (N + 1)$ tridiagonal transition matrix,

$$P = \begin{pmatrix} -\tilde{\lambda}_0 & \tilde{\lambda}_0 & & & & & \\ \tilde{\mu}_1 & -(\tilde{\lambda}_1 + \tilde{\mu}_1) & \tilde{\lambda}_1 & & & & \\ & \tilde{\mu}_2 & & -(\tilde{\lambda}_2 + \tilde{\mu}_2) & & & \\ & & & & \ddots & & \\ & & & & & \ddots & \\ & & & & & & \tilde{\lambda}_{N-2} \\ & & & & & & \tilde{\mu}_{N-1} & -(\tilde{\lambda}_{N-1} + \tilde{\mu}_{N-1}) & \tilde{\lambda}_{N-1} \\ & & & & & & & \tilde{\mu}_N & -\tilde{\mu}_N \end{pmatrix}. \quad (2)$$

Together with the initial condition $\mathbf{s}_0 = \mathbf{s}(0)$, Eq. (1) describes the exact dynamics of the continuous-time Markovian ε -SIS process on the complete graph K_N , which can be solved to find

$$\mathbf{s}^T(\tilde{t}) = \mathbf{s}_0^T e^{P\tilde{t}}. \quad (3)$$

Using the probability vector of the number of infected nodes $\mathbf{s}(\tilde{t})$ at time \tilde{t} , one may compute the average fraction of infected cases $y(\tilde{t})$, commonly known as the *prevalence*, as

$$y(\tilde{t}) = \frac{1}{N} \sum_{k=0}^N k s_k(\tilde{t}). \quad (4)$$

In the remainder of this work, we omit the tilde for the scaled time \tilde{t} for readability.

We intend to show that metastability in the ε -SIS process is directly linked to the eigenvalues of the transition matrix P . We start by denoting the eigenvalues ξ_1, \dots, ξ_{N+1} , the right-eigenvectors $\mathbf{v}_1, \dots, \mathbf{v}_{N+1}$, and the left-eigenvectors $\mathbf{w}_1, \dots, \mathbf{w}_{N+1}$ of the $(N + 1) \times (N + 1)$ transition matrix P . The eigenvalues of the transition matrix P are real, because P

is similar to a symmetric matrix \tilde{P} and similarity preserves the eigenvalues. The transformed matrix \tilde{P} is computed in Appendix A. The eigenvalues of P and \tilde{P} cannot be computed analytically for $N > 4$ because it involves finding the roots of a characteristic polynomial with degree N . Thus one resorts to numerical methods to obtain the eigenvalues. Once the eigenvalues are known, the corresponding eigenvectors can be computed analytically (Ref. [32], Appendix A.6.3).

Since all eigenvalues are real-valued, we may rank them in decreasing order $\xi_1 \geq \xi_2 \geq \dots \geq \xi_{N+1}$. Given that the tridiagonal matrix \tilde{P} is symmetric and all off-diagonal terms are nonzero,¹ all eigenvalues of P are distinct (Ref. [33], Lemma 7.7.1). The same conclusion follows by computing the probability generating function of the ε -SIS process and concluding that the resulting differential equation is of Sturm-Liouville type [21], which is known to have simple eigenvalues. The

¹Here, we assume that the curing rate δ , the effective infection rate τ and the effective self-infection rate ε^* are nonzero.

transition matrix P of the ε -SIS Markov chain has a unique, largest eigenvalue $\xi_1 = 0$, which corresponds to the steady state π . The remaining eigenvalues ξ_2, \dots, ξ_{N+1} are negative and distinct. The solution (3) can be written as

$$\mathbf{s}(t) = \pi + \sum_{k=2}^{N+1} c_k e^{\xi_k t} \mathbf{w}_k, \quad (5)$$

where ξ_k is the eigenvalue corresponding to the right-eigenvector \mathbf{w}_k of the ε -SIS process, and the constant $c_k = \mathbf{v}_k^T \mathbf{s}(0)$ projects the initial vector $\mathbf{s}(0)$ on the k th left-eigenvector \mathbf{v}_k [Ref. [11], Eq. (2.5)]. The vector $\mathbf{s}(t)$, whose components $s_k(t)$ specify the probability that k nodes at time t are infected, is decomposed in Eq. (5) into $N + 1$ eigenstates of which the corresponding eigenvectors $\mathbf{w}_1, \dots, \mathbf{w}_{N+1}$ span the $N + 1$ vector space. Each eigenvector \mathbf{w}_k in Eq. (5) is weighted by the coefficient $c_k e^{\xi_k t}$. The eigenvalue ξ_k resembles a rate and has units 1/time. The contribution of eigenvector \mathbf{w}_k to the solution $\mathbf{s}(t)$ decays exponentially over time with a decay rate equal to the eigenvalue ξ_k (the contribution decays because $\xi_k < 0$). The eigenvalue ξ_k is thus inversely proportional to the average time that the corresponding eigenvector \mathbf{w}_k significantly contributes to the solution $\mathbf{s}(t)$.

In particular, the second-largest eigenvalue ξ_2 (sometimes called the *convergence rate*, spectral gap, mixing rate, or decay parameter) is inversely proportional to the average time required to converge toward the steady state [25,34]. The convergence rate for continuous-time Markov chains and BDPs is thoroughly analyzed in probability theory. For an overview of bounds of the convergence rate in Markov chains and BDPs, we refer the reader to Van Doorn *et al.* [35] and Artalejo [25] and references therein. If the effective self-infection rate $\varepsilon^* = 0$, then the average time of convergence $E[T_{\text{extinction}}] = -1/\xi_2$ to the steady state (or equivalently, the *extinction time*, survival time, or absorption time) on the complete graph has the following exact relationship [27]:

$$E[T_{\text{extinction}}] = \sum_{i=1}^N \sum_{j=0}^{i-1} \frac{(N-i+j)!}{i(N-i)!} \tau^j.$$

Nearly all works consider the SIS process without self-infections. Most proofs for the convergence rate (e.g., the proof in [27]) are based on the hitting time distribution of the absorbing state. By introducing the self-infection process, the absorbing state no longer exists and the proofs therefore do not hold for the ε -SIS process. Fortunately, the introduction of the self-infection process makes the Markov chain of the ε -SIS process irreducible, implying that the steady state exists and is also unique. The existence of the steady state greatly simplifies the analysis of the ε -SIS process for large times, because we can analyze the behavior of the conceptually simpler steady state instead of the more complicated metastable state.

III. METASTABILITY IN THE ε -SIS PROCESS

Our primary motivation for researching the eigenvalues of the transition matrix P in Eq. (2) is the observation of plateau-behavior in the ε -SIS process [21], which is illustrated

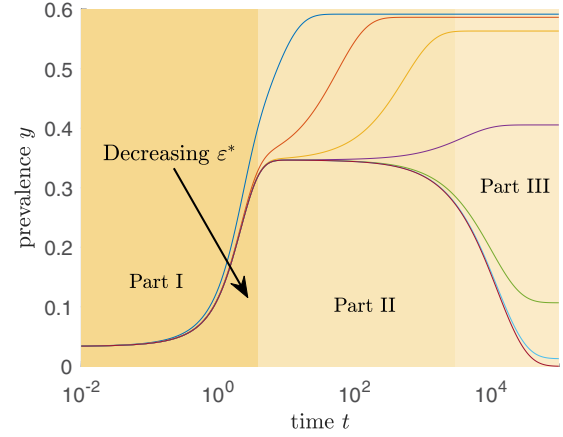


FIG. 2. Plateau-behavior in the Markovian ε -SIS process on the complete graph. Each curve is computed using the exact solution (5), and the parameters are $N = 30$ nodes, effective infection rate $\tau = 2.5\tau_c^{(1)} = 2.5/(N-1)$, the process starts with a single infected node, and the effective self-infection rate $\varepsilon^* = \{10^{-2}, 10^{-3}, 10^{-4}, 10^{-5}, 10^{-6}, 10^{-7}, 0\}$. For $\varepsilon^* \leq 10^{-5}$, the background colors indicate the current phase of the ε -SIS process: (I) initial phase, (II) metastable behavior, and (III) convergence to the steady state.

in Fig. 2. Each curve in Fig. 2 is computed based on the exact solution (5), where initially a single node is infected. For small effective self-infection rates $\varepsilon^* \leq 10^{-5}$, Fig. 2 depicts roughly three regimes for the time-varying prevalence: (I) initial phase, (II) metastable behavior, and (III) convergence to the steady state. Phase (I) is characterized by the fast convergence to the metastable state. In the metastable phase (II), the prevalence y stays nearly constant for an extended period of time. Finally, phase (III) shows the exponential convergence to the steady state π .

Plateau-behavior is generally caused by metastability of the dynamical process, where the infection and curing processes are temporarily in equilibrium (the physical explanation is presented in [7]). We consider the following definition of metastability for general dynamical processes that possess a steady state π .

Definition III.1. A dynamical process is *metastable* if the process stays in a certain state for an extended period of time before converging to the steady state π .

We quantify metastability for the ε -SIS process using the eigenvalue ratio, which was first introduced by Jacquez and Simon (Ref. [8], p. 85).

Definition III.2. The *eigenvalue ratio* ρ is defined as

$$\rho = \frac{\xi_3}{\xi_2}. \quad (6)$$

The eigenvalue ratio ρ is an indicator for the existence of plateaus [8]. If the eigenvalue ratio ρ is large, then the second-largest eigenvalue ξ_2 is much larger than the other eigenvalues ξ_3, \dots, ξ_{N+1} . The influence of the right-eigenvectors $\mathbf{w}_2, \dots, \mathbf{w}_{N+1}$ on the solution $\mathbf{s}(t)$ in (5), weighted by the exponentials $e^{\xi_k t}$, will therefore converge much faster to zero for the eigenvalues ξ_3, \dots, ξ_{N+1} than for the second-largest eigenvalue ξ_2 .

The height of the plateaus in Fig. 2 equals the prevalence y , which is defined in Eq. (4). Plateau-behavior, as shown in Fig. 2, is only clearly observed if the steady-state prevalence y_∞ is sufficiently different from the prevalence in the metastable state and if the effective self-infection rate ε^* is sufficiently small. Our definition of metastability in the ε -SIS process is as follows:

Definition III.3. The ε -SIS process is *metastable* if the eigenvalue ratio $\rho \gg 1$ and the prevalence y_∞ in the steady state is sufficiently different from the prevalence in the metastable state.

We analyze the case when the metastable prevalence y and the steady-state prevalence y_∞ are equal in Appendix B. We find the power-law relation $\varepsilon^* \sim \tau^{-N}$ if τ is sufficiently larger than the epidemic threshold τ_c . For further details, see Appendix B.

If the ε -SIS process is metastable, the average time spent in the metastable state is roughly equivalent to the average time required to converge to the steady state, because the average time between the onset of the disease and the arrival at the metastable state is relatively short (see Fig. 2 for an example).

IV. MEAN-FIELD APPROXIMATION OF THE ε -SIS PROCESS

The majority of the research on epidemiology is based on mean-field approximations of stochastic processes. However, the behavior of the Markovian ε -SIS process is intrinsically different from its mean-field approximation, especially regarding the metastable state. Recently, Prasse *et al.* [36] solved the continuous-time mean-field SIS process on the complete graph K_N with arbitrary initial conditions. We derive a similar result in Theorem IV.1 for the ε -SIS process with self-loops, whereby we added the infection rates τ_{ii} from each node i to itself. We refer to Appendix C for the derivation of the mean-field equations, which approximate the exact, Markovian solution $\mathbf{s}(t)$ by the mean-field state vector $\mathbf{s}_{\text{MF}}(t)$.

Theorem IV.1. Consider the mean-field approximation of the ε -SIS process on the complete graph with homoge-

neous transition rates and self-loops, given by Eq. (C2) in Appendix C, with arbitrary initial conditions. Then the viral state $\mathbf{s}_{\text{MF}}(t)$ is equal to

$$\mathbf{s}_{\text{MF}}(t) = c_1(t)\mathbf{z}_1 + c_2(t)\mathbf{z}_2 \quad (7)$$

at every time t . Here, \mathbf{z}_1 and \mathbf{z}_2 are orthonormal agitation modes, which are given by

$$\mathbf{z}_1 = \frac{1}{\sqrt{N}}\mathbf{u}, \quad (8)$$

where $\mathbf{u} = (1, \dots, 1)^T$ denotes the $N \times 1$ all-one vector, and

$$\mathbf{z}_2 = \|(I - \mathbf{z}_1\mathbf{z}_1^T)\mathbf{s}_{\text{MF}}(0)\|_2^{-1}(I - \mathbf{z}_1\mathbf{z}_1^T)\mathbf{s}_{\text{MF}}(0). \quad (9)$$

The functions $c_l(t) = \mathbf{z}_l^T \mathbf{s}_{\text{MF}}(t) \in \mathbb{R}$, where $l = 1, 2$, are the projection of the viral state vector $\mathbf{s}_{\text{MF}}(t)$ on the agitation mode \mathbf{z}_l . The scalar function $c_1(t)$ equals

$$c_1(t) = \frac{1}{2\tau\sqrt{N}} \left[\tau N - 1 - \varepsilon^* + w_{\varepsilon^*} \tanh\left(\frac{w_{\varepsilon^*}}{2}t + \Upsilon_{1,\varepsilon^*}(c_1(0))\right) \right]$$

with the *viral slope*

$$w_{\varepsilon^*} = \sqrt{(1 + \varepsilon^* - \tau N)^2 + 4\varepsilon^*\tau N}$$

and the constant

$$\begin{aligned} &\Upsilon_{1,\varepsilon^*}(c_1(0)) \\ &= \operatorname{arctanh}\left(\frac{1}{w_{\varepsilon^*}}(2\tau\sqrt{N}\mathbf{z}_1^T \mathbf{s}_{\text{MF}}(0) - \tau N + 1 + \varepsilon^*)\right). \end{aligned}$$

The scalar function $c_2(t)$ equals

$$\begin{aligned} c_2(t) &= \Upsilon_{2,\varepsilon^*}(c_2(0)) \exp\left(-\frac{1 + \varepsilon^* + \tau N}{2}t\right) \\ &\times \operatorname{sech}\left(\frac{w_{\varepsilon^*}}{2}t + \Upsilon_{1,\varepsilon^*}(c_1(0))\right), \end{aligned}$$

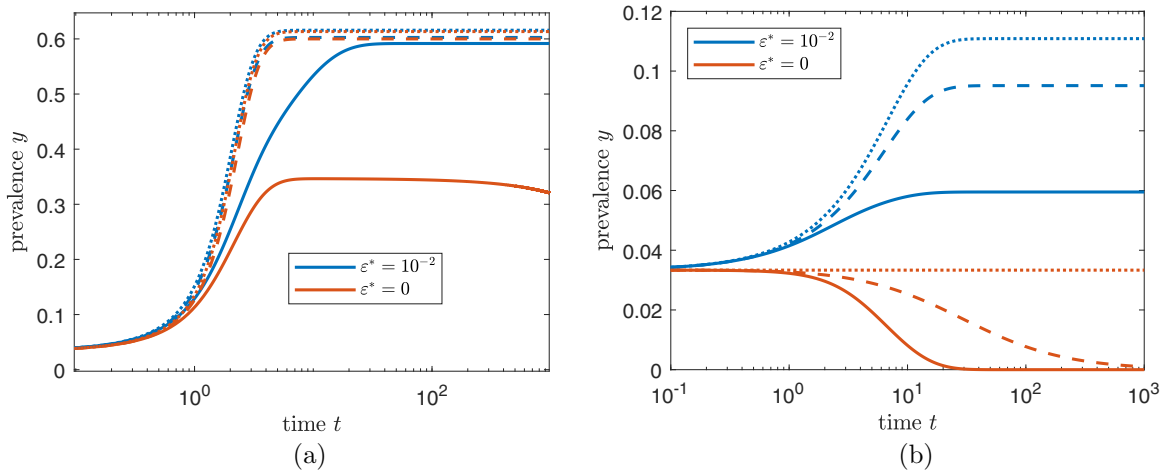


FIG. 3. The exact Markovian solution (solid lines), the mean-field approximation without self-loops (dashed lines), and exact mean-field solution with self-loops from Theorem IV.1 (dotted lines) of the ε -SIS process on the complete graph with $N = 30$ nodes for various effective self-infection rates ε^* for (a) effective infection rate $\tau = 2.5/(N - 1)$ and (b) effective infection rate $\tau = 1/(N - 1)$. The mean-field approximation is generally a loose upper bound for the Markovian ε -SIS dynamics.

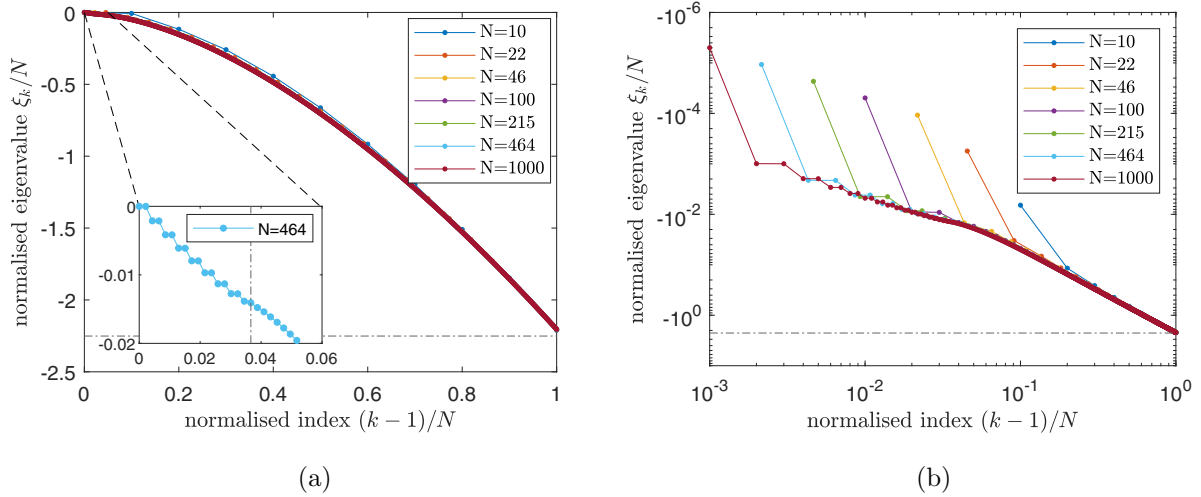


FIG. 4. All eigenvalues ξ_k of the transition matrix P on the complete graph with effective infection rate $\tau = 2/(N - 1)$, and effective self-infection rate $\varepsilon^* = 0.01/N$ on (a) linear-linear scale and (b) log-log scale for $k = 1, \dots, N + 1$. The eigenvalues have been normalized with respect to the number of nodes N . Normalized index 0 corresponds to the largest eigenvalue $\xi_1 = 0$, and normalized index 1 corresponds to the smallest eigenvalue ξ_{N+1} . The horizontal dash-dotted line indicates the lower bound for ξ_{N+1} from Theorem V.1. The largest eigenvalue $\xi_1 = 0$ is not shown in (b) because of the logarithmic axis. The inset in (a) zooms in for $0 \leq (k - 1)/N \leq 0.05$ and shows the critical index k_2 as a vertical dash-dotted line. In this case, the critical index $k_1 = 0$.

with the constant

$$\Upsilon_{2,\varepsilon^*}(c_2(0)) = \mathbf{z}_2^T \mathbf{s}_{\text{MF}}(0) \cosh(\Upsilon_{1,\varepsilon^*}(c_1(0))). \quad (10)$$

Proof. See Appendix C. ■

As derived in Appendix C, the mean-field prevalence upperbounds the Markovian prevalence $y(t)$. Theorem IV.1 states that the mean-field dynamics on the complete graph can be reduced from N equations to two agitation modes, where one is related to the initial condition and the other to the steady state. Hence, the metastable state [Phase (II) in Fig. 2] does not exist under the mean-field approximation, because the existence of only two agitation modes does not allow for an intermediate, transient regime.

We plot the Markovian prevalence, the mean-field prevalence and the mean-field prevalence with self-loops, based on Theorem IV.1, in Fig. 3. Figure 3 illustrates that the mean-

field approximation vastly overestimates the time-dependent fraction of infected nodes of the Markovian ε -SIS process, both with and without self-loops. If the effective infection rate τ is larger than the epidemic threshold τ_c , Fig. 3(a) shows that, for $N = 30$, the discrepancy between the mean-field prevalence and the Markovian prevalence is large everywhere, except at very small timescales or if ε^* is very large. Figure 3(b) is situated around the epidemic threshold τ_c , where the mean-field approximation is known to have the worst accuracy [18]. In the limit $N \rightarrow \infty$, the mean-field approximation error converges to zero, which we further illustrate in Sec. VIC. Given that the metastable state is a key epidemiological quantity and that the metastable state does not exist under the mean-field approximation, we focus in the remainder of this work on the Markovian ε -SIS process.

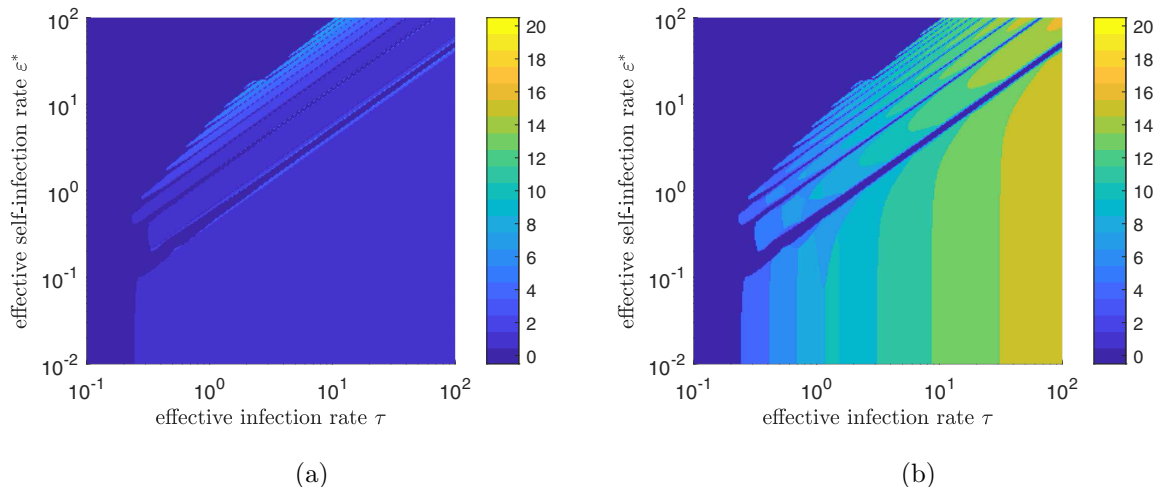


FIG. 5. The critical indices k_1 (a) and k_2 (b) for different values of the effective infection rate τ and the effective self-infection rate ε^* on the complete graph K_N with $N = 20$ nodes.

In addition to approximating the Markovian ε -SIS process by a mean-field approximation, various other approximation methods exist. We investigate an eigenmode approximation of the Markovian ε -SIS process on K_N in Appendix D. Unfortunately, for an accurate approximation, the number of eigenmodes scales proportional to the number of nodes N , rendering the approximation method infeasible for large networks.

V. SPECTRUM ANALYSIS OF THE ε -SIS PROCESS

Since the eigenvalues ξ_k are key for the characteristic timescales of the ε -SIS process, we focus on the determination of the eigenvalues ξ_k of the transition matrix P from Eq. (2). The eigenvalues are computed in several parameter limits in Theorem V.1.

Theorem V.1. The eigenvalues ξ_k of the transition matrix P satisfy²

$$\begin{aligned} \text{for } \varepsilon^* \rightarrow \infty, \quad \xi_k &= -(k-1)\varepsilon^* - (k-1)[\tau(N+1-k) + 1] + O\left(\frac{1}{\varepsilon^*}\right), \\ \text{for } \tau \rightarrow \infty, \quad \xi_k &= \begin{cases} -\frac{1}{4}\tau(N-1)(N+1) \pm \sqrt{\tau(N+1)}\sqrt{\frac{N-1}{2}} + O(1) & \text{if } N \text{ odd, } k = \frac{N+2\pm 1}{2}, \\ -\tau\left(\frac{N}{2}-1\right)\left(\frac{N}{2}+1\right) + \frac{N^3}{12} + \frac{N^2}{12} - \frac{5N}{6} - \frac{1}{3} \\ \pm \sqrt{1 + \left(\frac{N}{2}\right)^3\left(\frac{N}{2}+1\right)^2\left(\frac{N}{2}-1\right)} + O\left(\frac{1}{\sqrt{\tau}}\right) & \text{if } N \text{ even, } k = \frac{N+2\pm 2}{2}, \varepsilon^* = 1, \\ -\tau(k-1)(N-k+1) \\ + (-\varepsilon^*(N-k+1) + \frac{(k-1)(N-k+1)(N+1)}{(2k-N-3)(2k-N-1)}) + O\left(\frac{1}{\sqrt{\tau}}\right) & \text{otherwise,} \end{cases} \\ \text{for } \varepsilon^* < \frac{1}{N}, \quad \xi_{N+1} &\gtrsim \begin{cases} -\left(\frac{1}{2x} + 1 + \frac{x}{2}\right)N & \text{for } x \geq 1, \\ -2N & \text{for } x < 1, \end{cases} \end{aligned}$$

for $k = 1, 2, \dots, N + 1$ and where $x = \tau/\tau_c^{(1)}$ is the normalized effective infection rate.

Proof. See Appendix E. ■

Theorem V.1 states that the eigenvalue ratio ρ for large effective self-infection rates ε^* equals $\rho = \xi_3/\xi_2 \approx 2$. Thus metastability is not expected if the self-infection process dominates the infection and curing processes. For large but finite effective infection rates τ and effective self-infection rates ε^* , the asymptotic expansions in Theorem V.1 are only valid if the second term is strictly smaller than the first term, the third is smaller than the second, etc. For example, the second term in the expansion $\tau \rightarrow \infty$ must be strictly smaller than the first term, which only holds if $\tau > N + 1$ (see Appendix E for the derivation). Hence, the expansions in Theorem V.1 provide valuable insights into the eigenvalues ξ_k , even for finite values of the effective infection rate τ and effective self-infection rate ε^* .

We present here a full numerical analysis of the eigenvalues for finite parameter values. We compute the eigenvalues of the transition matrix P in MATLAB using the command `eig`. Figure 4 illustrates the normalized eigenvalues ξ_k/N versus the normalized index $(k-1)/N$ of the ε -SIS process for $k = 1, \dots, N + 1$. An interesting observation from Fig. 4(a) is the negligible dependence of the network size N on the normalized eigenvalues ξ_k/N . We further investigate the influence of the network size N by simulations in Sec. VI. Figure 4(b) shows that the second-largest eigenvalue ξ_2 deviates significantly from the other eigenvalues ξ_3, \dots, ξ_{N+1} . The difference between the second-largest eigenvalue ξ_2 and the third-largest

eigenvalue ξ_3 is the precise reason why we used the eigenvalue ratio ρ in our Definition III.3 of the metastable state in the ε -SIS process.

The inset of Fig. 4(a) shows a “staircase” for certain eigenvalues of the ε -SIS process. We propose to subdivide the eigenvalues into three regimes. We *define* the critical index k_1 as the start of the staircase, and the critical index k_2 as the end of the staircase. If the staircase does not exist, we take $k_1 = k_2 = 0$. The main plot of Fig. 4(a) illustrates that the eigenvalues ξ_k with $k > k_2$ roughly follow a quadratic relation between the normalized eigenvalues ξ_k/N and the normalized

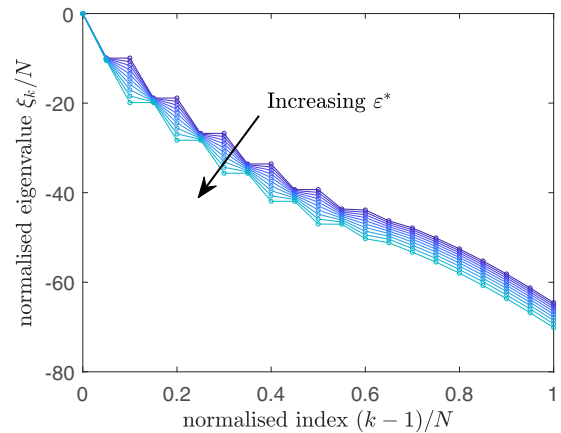


FIG. 6. The normalized eigenvalues ξ_k/N on the complete graph K_N with $N = 20$ nodes and $\tau = 10$ for different effective self-infection rates between $\varepsilon^* = 10$ and $\varepsilon^* = 20$. By varying the effective self-infection rate ε^* , one eigenvalue of the nearly degenerate pair changes significantly, whereas the other remains largely unchanged.

²Contrary to our general consensus that the eigenvalues $0 = \xi_1 > \xi_2 > \dots > \xi_{N+1}$ are ordered, the eigenvalues ξ_k in Theorem V.1 are not necessarily ordered.

index $(k-1)/N$. Theorem V.1 states that the eigenvalues ξ_k converge to $\tau(k-1)(N-k+1)$ if the effective infection rate τ tends to infinity, which explains the nearly quadratic form for $k > k_2$. On the other hand, the inset of Fig. 4(a) shows staircase behavior for $k_1 < k \leq k_2$. The staircase is the result of two nearly degenerate (but strictly distinct) eigenvalues of the ε -SIS process. If the effective infection rate τ tends to infinity, the eigenvalues converge to $\xi_k \rightarrow \tau(k-1)(N-k+1)$, which are degenerate because $\xi_k = \xi_{N-k+2}$ for all $k = 1, \dots, N+1$. Even for large, finite effective infection rates τ , there is a small region $k_1 < k \leq k_2$ where staircase behavior is observed, which is illustrated in Fig. 4.

The staircase behavior from Fig. 4(a) is not always observed. Figure 5 illustrates the dependence of the critical indices k_1 and k_2 on the effective infection rate τ and the effective self-infection rate ε^* . Staircases are observed if the critical index $k_2 > 0$ in Fig. 5, whereas the critical index k_1 indicates the start of the staircase and is only nonzero for a small region in the (τ, ε^*) -space. If the effective infection rate τ is below

the epidemic threshold τ_c , both indices $k_1 = k_2 = 0$ and no staircases can be observed. In the limit $\varepsilon^* \rightarrow \infty$, Theorem V.1 shows that staircases do not exist, because $\xi_k \rightarrow -(k-1)\varepsilon^*$ for $k = 1, \dots, N+1$. In the intermediate regime, where $0 < \varepsilon^* < \infty$ and $\tau > \tau_c$, the critical index k_2 is often nonzero, indicating staircase behavior. However, Fig. 5 additionally shows small blue regions, where staircase behavior is not observed. The blue regions are centered around $\varepsilon^* = \tau(n + \frac{1}{2})$, where $n = 0, 1, 2, \dots$. Upon further inspection, the staircases seem best visible for $\varepsilon^* = \tau n$, where $n = 1, 2, \dots$.

For a given number of k infected nodes, the total effective infection rate equals $\tau k(N-k)$ and the total effective self-infection rate $\varepsilon^*(N-k)$. The effect of both infection processes is equally strong if its rates are equal, which implies that $\varepsilon^* = \tau k$. Thus, the staircases are best visible if the total rate of the infection process and self-infection process are equally large. We argue that one eigenvalue of the nearly degenerate pair is due to the infection process and one eigenvalue corresponds to the self-infection process. Then,

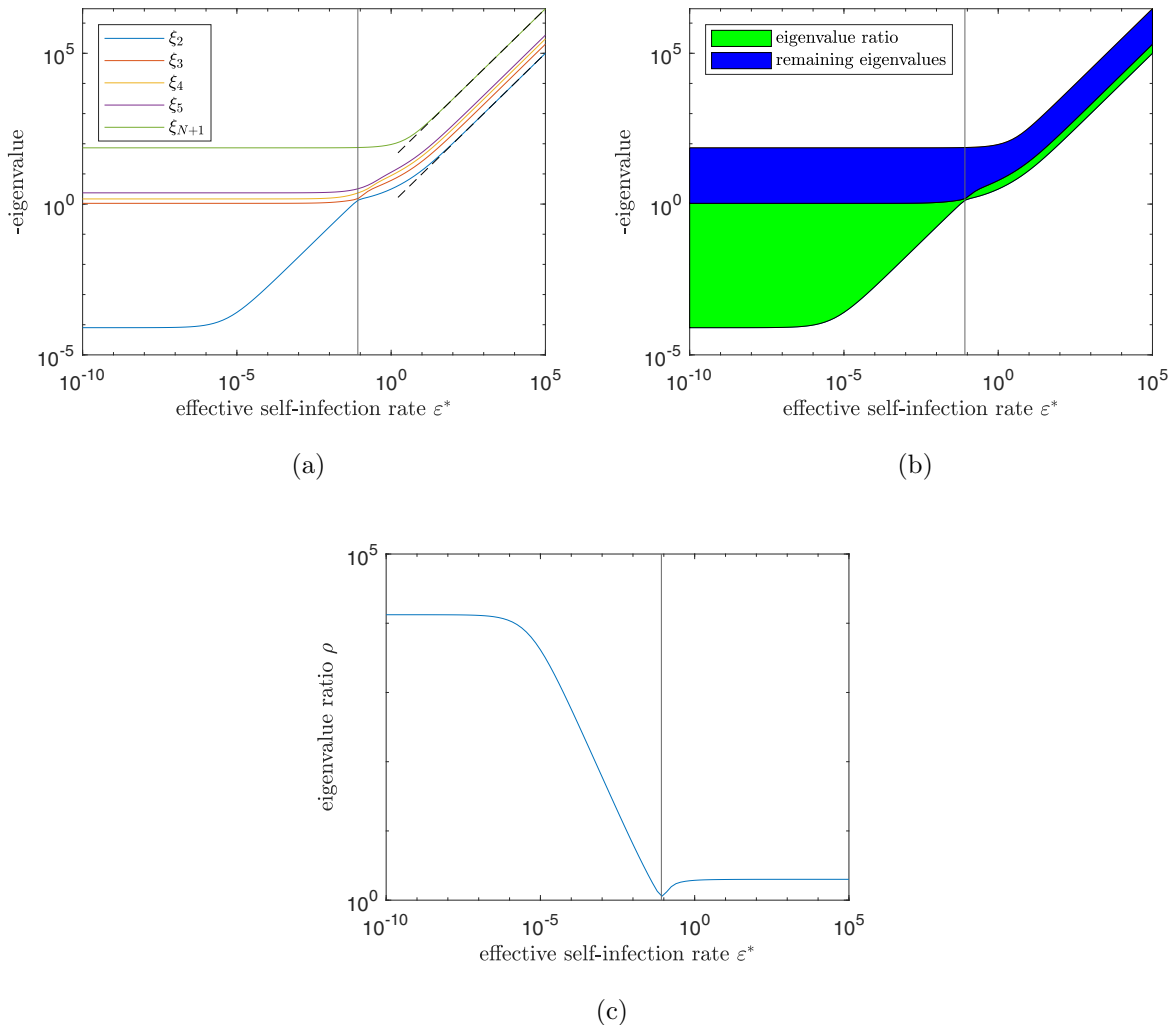


FIG. 7. The eigenvalues of the transition matrix P for the complete graph with $N = 30$ nodes and effective infection rate $\tau = 2.5\tau_c^{(1)}$ for varying effective self-infection rates ε^* on a log-log scale. Subfigure (a) shows the second-to-fifth-largest eigenvalues $\xi_2, \xi_3, \xi_4, \xi_5$ and smallest eigenvalue ξ_{N+1} as a function of the effective self-infection rate ε^* . The vertical line indicates the relation $\varepsilon^* = \tau$. Subfigure (b) is equivalent to (a), but here the eigenvalue ratio ρ is colored green (light) and the area with the other eigenvalues is colored blue (dark). Finally, (c) shows a plot of the eigenvalue ratio ρ vs the effective self-infection rate ε^* .

by varying either τ or ε^* , one of the eigenvalues of the pair must remain unchanged. Figure 6 shows the normalized eigenvalues for varying effective self-infection rates ε^* between τ and 2τ . Indeed, while the effective self-infection rate ε^* is varied, one eigenvalue of the nearly degenerate pair changes whereas the other stays approximately constant. Thus, a plausible explanation for the staircase behavior is a balance between self-infections and infections between nodes. While Fig. 6 supports our explanation for the staircase behavior, an analytic proof remains an open research question.

To summarize, we believe that the eigenvalues ξ_k in the regime $2 < k \leq k_1$ are related to self-infection-dominated behavior, the regime $k_1 < k \leq k_2$ describes when the influence of the infection and self-infection process is equally strong, and the regime $k > k_2$ pertains to the infection-dominated behavior. Equation (11) summarizes our findings for the eigenvalues ξ_k of the ε -SIS process:

$$\xi_k \approx \begin{cases} 0 & \text{for } k = 1, \\ \text{convergence rate} & \text{for } k = 2, \\ \text{roughly linear} & \text{for } 2 < k \leq k_1, \\ \text{staircases} & \text{for } k_1 < k \leq k_2, \\ \text{roughly quadratic} & \text{for } k_2 < k \leq N + 1. \end{cases} \quad (11)$$

VI. NUMERICAL SIMULATIONS

We perform numerical simulations to examine how the entire set of eigenvalues changes with the effective self-infection rate ε^* the effective infection rate τ and the network size N .

A. The influence of the effective self-infection rate ε^*

First, we examine the influence of the effective self-infection rate ε^* on the eigenvalues by fixing the network size N and the effective infection rate τ . Figure 7 shows the absolute value of the eigenvalues of the transition matrix P for varying effective self-infection rates ε^* .

The ε -SIS process is governed by two infection processes: the infection process and the self-infection process. All events in the continuous-time Markovian ε -SIS process are independent, such that the rate to transition from a completely susceptible population to one infected node is solely governed by the self-infection process and may happen for every node independently, leading to a total rate ε^*N . Simultaneously, if a single node is infected, another node is infected with rate $\tau(N - 1)$. If $\varepsilon^*N < \tau(N - 1)$, the process is dominated by the infection process, whereas the process is dominated by self-infections if $\varepsilon^*N > \tau(N - 1)$. For large network sizes N , the influence of the self-infection process and the infection process is equally large if $\tau \approx \varepsilon^*$. The vertical line in Fig. 7 indicates the relation $\tau = \varepsilon^*$. The minimum of the eigenvalue ratio ρ and the relation $\tau = \varepsilon^*$ coincide in Fig. 7(c). At the intersection point $\tau = \varepsilon^*$, the minimal eigenvalue ratio ρ is approximately 1. Then both eigenvalues are approximately equal and exhibit staircases in the eigenvalue spectrum, which was discussed in detail in Sec. V.

The second-largest eigenvalue ξ_2 changes significantly from $\varepsilon^* = 0$ to $\varepsilon^* = \tau$, but the remaining eigenvalues ξ_3, \dots, ξ_{N+1} stay nearly constant. To the right of the vertical line in Fig. 7, the remaining eigenvalues increase as well. In the limit of large effective self-infection rates ε^* , it holds

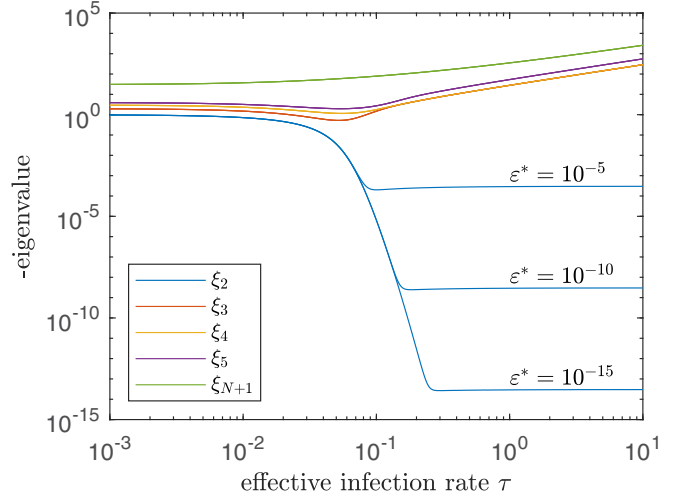


FIG. 8. Illustration of the explosive phase transition for effective self-infection rates $\varepsilon^* > 0$ and no phase transition for $\varepsilon^* = 0$ for the second-largest eigenvalue ξ_2 . The remaining eigenvalues ξ_3, \dots, ξ_{N+1} are nearly indistinguishable for different ε^* . The network size equals $N = 30$.

that $\xi_k \approx -(k - 1)\varepsilon^*$ according to Theorem V.1. The smallest eigenvalue $\xi_{N+1} \approx -\varepsilon^*N$ and the second-largest eigenvalue $\xi_2 \approx -\varepsilon^*$ are shown by dashed lines in Fig. 7. Thus, the eigenvalues ξ_k increase linearly with the effective self-infection rate ε^* , because the self-infection process dominates the other processes and drives the ε -SIS process to the all-infected state.

If the effective self-infection rate $\varepsilon^* < \tau$, Fig. 7 shows that the self-infection process barely influences the characteristic timescales of the ε -SIS process, which was also observed in Fig. 2. A seemingly contradictory result was recently obtained by Van Mieghem [7], who showed that the steady-state prevalence y_∞ exhibits an explosive phase transition at certain small effective self-infection rates ε^* . The difference is that we consider a fixed effective infection rate τ and vary the effective self-infection rate ε^* , which contrasts [7], where the effective infection rate τ is varied for fixed self-infection rates $\varepsilon^* = 0$ and $\varepsilon^* > 0$. Performing a similar analysis as [7] on the eigenvalues, Fig. 8 illustrates that the second-largest eigenvalue ξ_2 is heavily influenced by the effective self-infection rate ε^* . For any finite effective self-infection rate $\varepsilon^* > 0$, there exists a phase transition for some effective infection rate τ , where the second-largest eigenvalue ξ_2 converges to a constant for large effective infection rates τ . In the limit $\varepsilon^* \rightarrow 0$, no such transition is observed, which is in agreement with [7]. The other eigenvalues ξ_3, \dots, ξ_{N+1} remain largely unaffected by considering the limit $\varepsilon^* \rightarrow 0$.

B. The influence of the effective infection rate τ

Analogously to the effective self-infection rate ε^* , we analyze the influence of the effective infection rate τ on the eigenvalues of the transition matrix P in Fig. 9. The vertical line in Fig. 9 illustrates the mean-field epidemic threshold $\tau_c^{(1)} = \frac{1}{N-1}$, which is slightly smaller than the true epidemic threshold [9,37]. Below the epidemic threshold τ_c , the eigenvalue ratio ρ in Fig. 9(c) is small. Around the epidemic

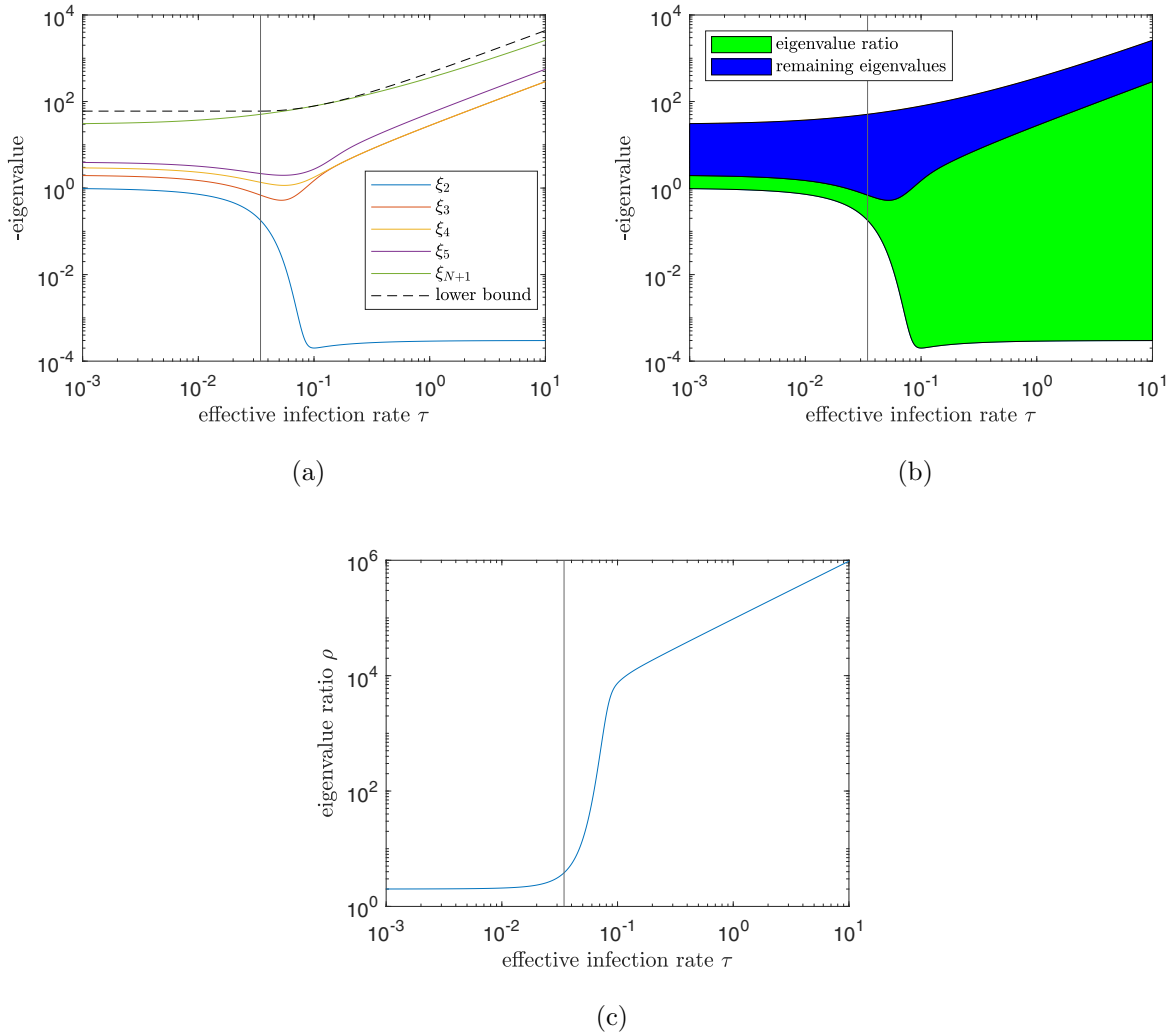


FIG. 9. The eigenvalues of the transition matrix P for the complete graph with $N = 30$ nodes and effective self-infection rate $\varepsilon^* = 10^{-5}$ for varying effective infection rates τ . Subfigure (a) shows the second-to-fifth-largest eigenvalues $\xi_2, \xi_3, \xi_4, \xi_5$ and smallest eigenvalue ξ_{N+1} as a function of the effective infection rate τ . The vertical line indicates the mean-field epidemic threshold $\tau_c^{(1)}$, which is slightly smaller than the true epidemic threshold τ_c . Subfigure (b) is equivalent to (a), but here the eigenvalue ratio ρ is colored green (light) and the area with the other eigenvalues is colored blue (dark). Finally, (c) shows a plot of the eigenvalue ratio ρ vs the effective infection rate τ . Finally, (a) illustrates the lower bound for the smallest eigenvalue ξ_{N+1} from Theorem V.1 by a dashed line.

threshold τ_c , the eigenvalue ratio ρ increases rapidly, as illustrated in Fig. 9(c).

For large effective infection rates τ , the second-largest eigenvalue ξ_2 converges to $-\varepsilon^*N$ whereas the remaining eigenvalues ξ_3, \dots, ξ_{N+1} increase linearly with the effective infection rate τ , which is in line with Theorem V.1. Hence, the eigenvalue ratio ρ tends to infinity if $\tau \rightarrow \infty$ and the system is considered metastable according to our Definition III.3. For large effective infection rates τ and starting with a nonzero number of infected nodes, the remaining nodes will be infected extremely quickly. The spreading is only slowed down by the transition from 0 to 1 infected node. The metastable state here is the all-healthy state, which takes a considerable amount of time to leave, whereafter the process converges extremely fast to the all-infected state. The convergence rate from the metastable state to the steady state, which equals minus the second-largest eigenvalue $-\xi_2$, exactly equals the

rate to jump from 0 to 1 infected node, which is given by the scaled birth rate $\tilde{\lambda}_0 = \varepsilon^*N$.

The epidemic threshold τ_c in the Markovian ε -SIS process exhibits a second-order phase transition.³ Van Mieghem and Cator (Ref. [13], p. 9) derived the following relation for the epidemic threshold τ_c for ε -SIS dynamics on the complete graph for large network sizes $N \gg 1$ and for small effective

³A first-order, abrupt phase transition at the epidemic threshold τ_c exhibits a discontinuity in the first derivative of the steady-state prevalence y_∞ . A second-order, continuous phase transition is an interval $[a, b]$ in which the behavior of the ε -SIS process gradually changes from nearly exponential die-outs to long-lived epidemic outbreaks.

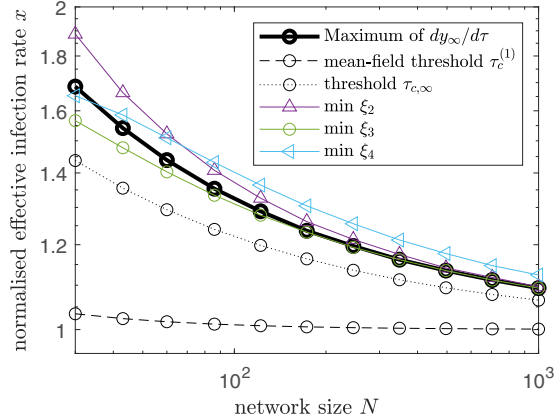


FIG. 10. Several formulas for the suggested epidemic threshold τ_c for various network sizes N .

self-infection rates $\varepsilon^* < \frac{1}{N}$:

$$\tau_{c,\infty} = \frac{1}{N + 2 - 2\sqrt{N + 1}}. \quad (12)$$

We expand both approximations for the epidemic threshold τ_c for large network sizes $N \gg 1$:

$$\begin{aligned} \tau_c^{(1)} &= \frac{1}{N-1} = \frac{1}{N} \left[1 + \frac{1}{N} + O\left(\frac{1}{N^2}\right) \right], \\ \tau_{c,\infty} &= \frac{1}{N + 2 - 2\sqrt{N + 1}} \\ &= \frac{1}{N} \left[1 + \frac{2}{\sqrt{N}} + \frac{2}{N} - \frac{1}{N\sqrt{N}} + O\left(\frac{1}{N^2}\right) \right]. \end{aligned}$$

Figure 9 illustrates that the eigenvalues ξ_2 , ξ_3 , and ξ_4 reach a minimum at a certain infection rate τ . We verify our hypothesis that the minimum of ξ_2 , ξ_3 , or ξ_4 coincides with the true epidemic threshold by plotting the mean-field threshold $\tau_c^{(1)}$, Van Mieghem and Cator's threshold $\tau_{c,\infty}$, and the numerically obtained effective infection rates τ for which the eigenvalues ξ_2 , ξ_3 and ξ_4 attain a minimum in Fig. 10. Additionally, we compute the steady-state prevalence y_∞ for the ε -SIS process, and we take the derivative of the steady-state prevalence y_∞ with respect to the effective infection rate τ . Then the epidemic threshold follows as the effective infection rate τ for which $dy_\infty/d\tau$ is maximal.⁴ The maximum of $dy_\infty/d\tau$ indicates for which effective infection rate τ the steady-state prevalence grows the fastest, which is presumably a good indicator of the epidemic threshold. Figure 10 depicts that the effective infection rate τ where the minimum ξ_3 is attained is very close to Van Mieghem and Cator's threshold based on the maximum of $dy_\infty/d\tau$. Interestingly, Van Mieghem and Cator's threshold $\tau_{c,\infty}$ is always larger than the mean-field threshold $\tau_c^{(1)}$, but always lower than the other estimates.

Figure 11 shows the steady-state prevalence y_∞ and the eigenvalue ratio ρ for varying infection rates τ . Above the epidemic threshold τ_c , the eigenvalue ratio ρ increases

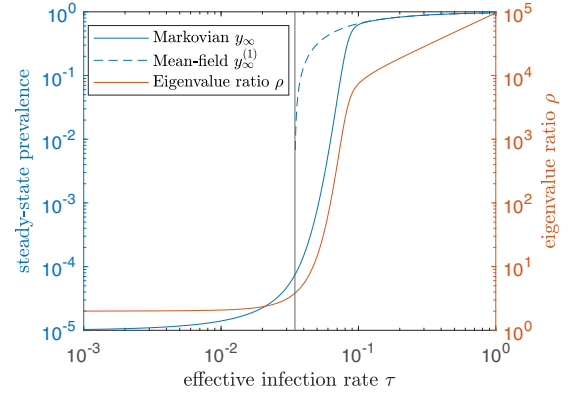


FIG. 11. The steady-state prevalence y_∞ , the mean-field steady-state prevalence $y_\infty^{(1)}$, and the eigenvalue ratio ρ with $N = 30$ nodes and effective self-infection rate $\varepsilon^* = 10^{-5}$ for varying effective infection rate τ . The vertical line indicates the mean-field epidemic threshold $\tau_c^{(1)} = \frac{1}{N-1}$, which is slightly smaller than the true epidemic threshold τ_c .

significantly and the time-dependent ε -SIS process will show metastable behavior. Below the epidemic threshold τ_c , metastability is never observed because the eigenvalue ratio ρ is small. We conclude here that the epidemic threshold τ_c not only describes for which infection rates τ the epidemic persists or dies out, but it is additionally a good descriptor of whether the ε -SIS process exhibits metastable behavior.

For noncomplete graphs, we expect that a similar conclusion will hold, but the 2^N -sized Markov chain for general graphs prevents us from rigorously demonstrating this claim. For connected Erdős-Rényi graphs with $N \leq 12$ nodes and a randomly chosen link-connectivity p , simulations indicate that the eigenvalue ratio ρ and the steady-state prevalence y_∞ show a similar plot as for the complete graph in Fig. 11.

C. The influence of the network size N

Finally, we investigate the effect of the network size N on the ε -SIS process. In the limit $N \rightarrow \infty$, the Markovian ε -SIS process exactly converges to the mean-field approximation [38]. Figure 12 shows the steady-state prevalence y_∞ for various network sizes and the mean-field prevalence $y_\infty^{(1)} = 1 - 1/x$. By increasing the network size N , the steady-state prevalence y_∞ converges to the mean-field approximation. One of the methods in Sec. VIB to estimate the epidemic threshold τ_c is based on the computation of the derivative $dy_\infty/d\tau$, which is plotted in Fig. 12(b). We estimate the epidemic threshold τ_c based on the peak of $dy_\infty/d\tau$, which converges to the mean-field threshold $x = 1$ if the network size N increases to infinity. All curves have a $1/x^2$ tail, which agrees with the mean-field steady-state prevalence $dy_\infty^{(1)}/d\tau = 1/x^2$.

We further investigate the eigenvalues of the ε -SIS process in Fig. 13, where we scale the effective infection rate τ/N and the effective self-infection rate ε^*/N . If the effective infection rate $\tau = 1.5\tau_c^{(1)}$ is larger than the epidemic threshold τ_c , as shown in Fig. 13(a), then by fixing k , all eigenvalues ξ_k converge to a constant value in the limit $N \rightarrow \infty$. For

⁴We further investigate the maximum of $dy_\infty/d\tau$ as a function of the network size N in Sec. VIC.

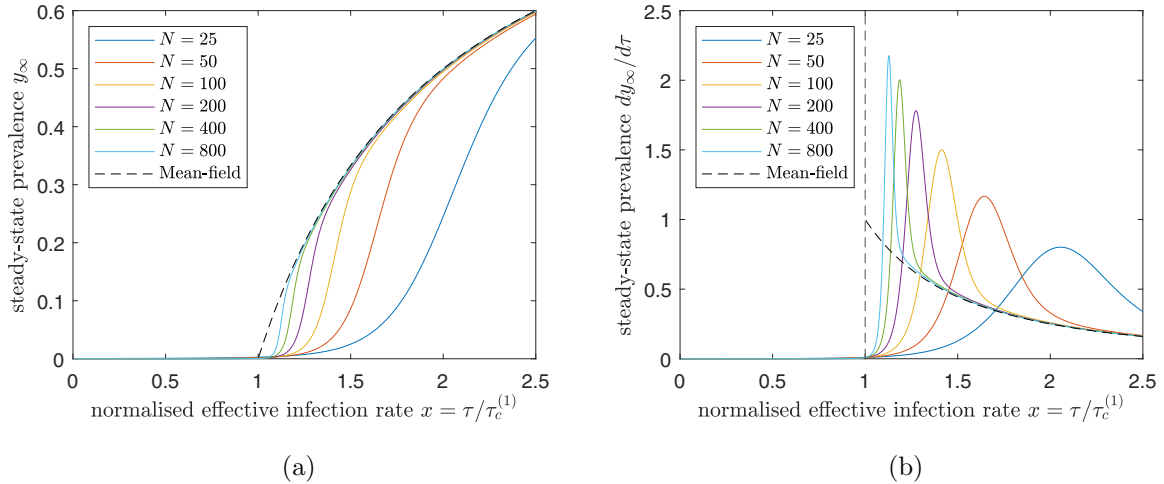


FIG. 12. The normalized effective infection rate $x = \tau/\tau_c^{(1)}$ vs the steady-state prevalence y_∞ for varying network sizes N and the mean-field steady-state prevalence $y_\infty^{(1)} = 1 - \frac{1}{x}$ and $\varepsilon^* = 0.01/N$.

example, the second-largest eigenvalue ξ_2 stays nearly constant for $N \gtrsim 100$. Closer to the epidemic threshold, namely for $\tau = 1.2\tau_c^{(1)}$ in Fig. 13(b), convergence occurs near $N \gtrsim 600$.

The mean-field approximation of the ε -SIS process is often used in network theory to reduce the computational complexity of the 2^N -sized Markov chain. In the limit of the network size N approaching infinity, the mean-field approximation becomes the exact solution, at least for the complete graph [38]. In practice, however, finite-sized networks are also approximated by mean-field methods, introducing an approximation error. It is known that mean-field methods perform poorly around the epidemic threshold, because the assumed independence of the stochastic variables does not hold. We illustrate here that around the epidemic threshold, the number of nodes N in the complete graph required to obtain a reasonable accuracy with the mean-field method tends to increase closer to the epidemic threshold.

We illustrate the aforementioned statement by focusing on the second-largest eigenvalue ξ_2 of the transition matrix P . We define the *critical network size* N_c as the smallest network size N for which the second-largest eigenvalue ξ_2 has a relative error of less than 10^{-6} compared to ξ_2 in the thermodynamic limit. Figure 14 exemplifies that the critical network size N_c increases if the epidemic threshold is approached from above.

VII. CONCLUSION

In this paper, we analyzed the continuous-time Markovian ε -SIS process on the complete graph with N nodes. The transition matrix corresponding to the underlying Markov chain has $N + 1$ distinct eigenvalues, of which the largest eigenvalue is zero and corresponds to the steady state and the remaining eigenvalues are all negative. Metastable behavior can be observed in the ε -SIS process if the ratio between the second-largest and third-largest eigenvalue of the transition matrix is sufficiently large. The remaining eigenvalues are nearly

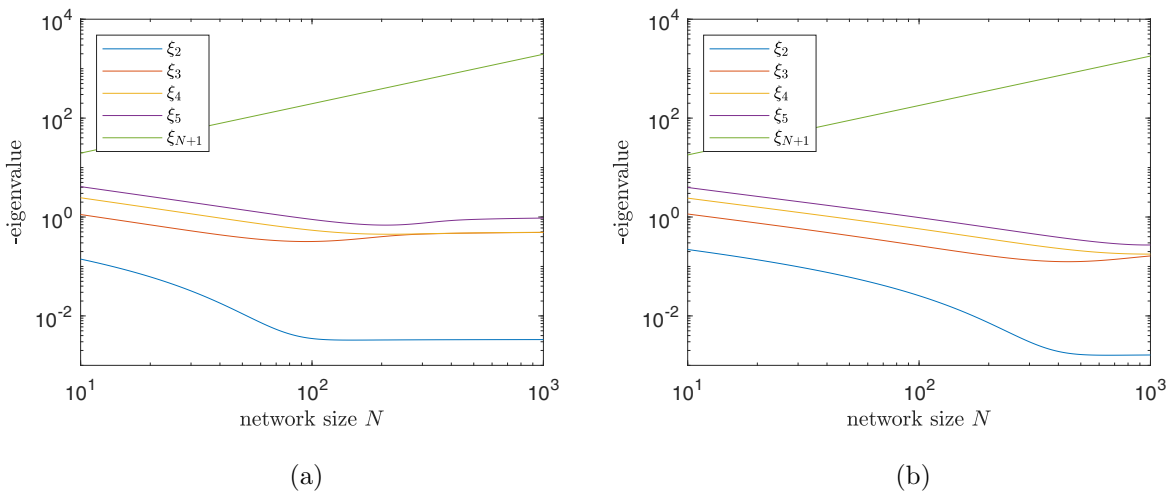


FIG. 13. The eigenvalues of the transition matrix P for the complete graph with effective self-infection rate $\varepsilon^* = 0.01/N$. Both subfigures show the second-to-fifth-largest eigenvalues $\xi_2, \xi_3, \xi_4, \xi_5$ and smallest eigenvalue ξ_{N+1} as a function of the network size N . Subfigure (a) corresponds to effective infection rate $\tau = 1.5\tau_c^{(1)} = 1.5/(N - 1)$ and (b) to $\tau = 1.2\tau_c^{(1)} = 1.2/(N - 1)$.

which implies that $\tilde{P} = HPH^{-1}$ is a symmetric matrix. The transformed matrix \tilde{P} equals

$$\tilde{P} = \begin{pmatrix} -\lambda_0 & \sqrt{\lambda_0\mu_1} & & & & & \\ \sqrt{\lambda_0\mu_1} & -(\lambda_1 + \mu_1) & \sqrt{\lambda_1\mu_2} & & & & \\ & \sqrt{\lambda_1\mu_2} & -(\lambda_2 + \mu_2) & \ddots & & & \\ & & & \ddots & & & \\ & & & & \ddots & & \\ & & & & & \sqrt{\lambda_{N-2}\mu_{N-1}} & -(\lambda_{N-1} + \mu_{N-1}) & \sqrt{\lambda_{N-1}\mu_N} \\ & & & & & \sqrt{\lambda_{N-1}\mu_N} & -\mu_N & \end{pmatrix}.$$

The transformed matrix \tilde{P} is symmetric and has therefore real eigenvalues. Since the similarity transform preserves the eigenvalues, we conclude that P has real eigenvalues.

For the numerical computation of the eigenvalues of the transition matrix P , the best practice is to consider the transformed matrix \tilde{P} instead of the original matrix P , because symmetric matrices have favorable properties for most eigenvalue algorithms [41]. We further improve the numerical procedure by removing the steady state π corresponding to the eigenvalue $\xi = 0$. Here, we follow Ref. [35] (Secs. 3 and 4). Given the transition matrix P , we define \bar{P} as the reduced $N \times N$ -matrix with entries $\bar{p}_{ij} = p_{ji} - p_{0i}$ for $i, j = 1, 2, \dots, N$. We now prove that the eigenvalues of \bar{P} are equal to the eigenvalues of P , except for the removed eigenvalue zero. Let ξ be an eigenvalue of P , and let $\mathbf{v} = (v_0, v_1, \dots, v_N)$ be the corresponding eigenvector. Furthermore, we denote \mathbf{u} as the $(N + 1) \times 1$ all-ones vector. Since $P\mathbf{u} = \mathbf{0}$, it follows that

$$\bar{P}^T(\bar{\mathbf{v}} - v_0\bar{\mathbf{u}}) = \xi(\bar{\mathbf{v}} - v_0\bar{\mathbf{u}}),$$

where $\bar{\mathbf{v}} = (v_1, \dots, v_N)$ and $\bar{\mathbf{u}}$ is the $N \times 1$ all-ones vector. Thus ξ is also an eigenvalue of \bar{P} , unless $\bar{\mathbf{v}} - v_0\bar{\mathbf{u}} = \mathbf{0}$, which is only true if $\bar{\mathbf{v}}$ is constant, thus corresponding to $\xi = 0$. Hence, the eigenvalues of \bar{P} equal the eigenvalues of P , and the matrix \bar{P} equals

$$\bar{P} = \begin{pmatrix} -(\lambda_0 + \lambda_1 + \mu_1) & \mu_2 - \lambda_0 & -\lambda_0 & \dots & -\lambda_0 & -\lambda_0 & -\lambda_0 \\ \lambda_1 & -(\lambda_2 + \mu_2) & \mu_3 & & & & \\ & & & \ddots & & & \\ & & & & \ddots & & \\ & & & & & \lambda_{N-2} & -(\lambda_{N-1} + \mu_{N-1}) & \mu_N \\ & & & & & & \lambda_{N-1} & -\mu_N \end{pmatrix}.$$

The reduced matrix \bar{P} can be transformed into a tridiagonal matrix. Let T be the upper triangular matrix with ones at and above the diagonal, and the remaining terms are zero. Then

$$T = \begin{pmatrix} 1 & 1 & 1 & \dots & 1 & 1 \\ & 1 & 1 & \dots & 1 & 1 \\ & & \ddots & & \vdots & \vdots \\ & & & \ddots & \vdots & \vdots \\ & & & & 1 & 1 \\ & & & & & 1 \end{pmatrix}, \quad T^{-1} = \begin{pmatrix} 1 & -1 & & & & \\ & 1 & -1 & & & \\ & & \ddots & \ddots & & \\ & & & 1 & -1 & \\ & & & & & 1 \end{pmatrix},$$

such that the reduced, transformed matrix $\bar{\bar{P}} = T\bar{P}T^{-1}$ equals

$$\bar{\bar{P}} = \begin{pmatrix} -(\lambda_0 + \mu_1) & \mu_1 & & & & & \\ \lambda_1 & -(\lambda_1 + \mu_2) & \mu_2 & & & & \\ & \lambda_2 & -(\lambda_2 + \mu_3) & \ddots & & & \\ & & & \ddots & & & \\ & & & & \ddots & & \\ & & & & & \lambda_{N-2} & -(\lambda_{N-2} + \mu_{N-1}) & \mu_{N-1} \\ & & & & & & \lambda_{N-1} & -(\lambda_{N-1} + \mu_N) \end{pmatrix}.$$

The reduced, transformed matrix $\bar{\bar{P}}$ is asymmetric and can be converted to a symmetric matrix $\bar{\bar{\bar{P}}}$ using the same transformation matrix H as for the original transition matrix P . The main advantages of the reduced, transformed, symmetric matrix $\bar{\bar{\bar{P}}}$ compared to the original transition matrix P are that numerical methods to obtain eigenvalues (i) are more efficient because the matrix is symmetric, (ii) prevent complex eigenvalues due to symmetry, and (iii) are less prone to rounding errors as the zero eigenvalue is removed.

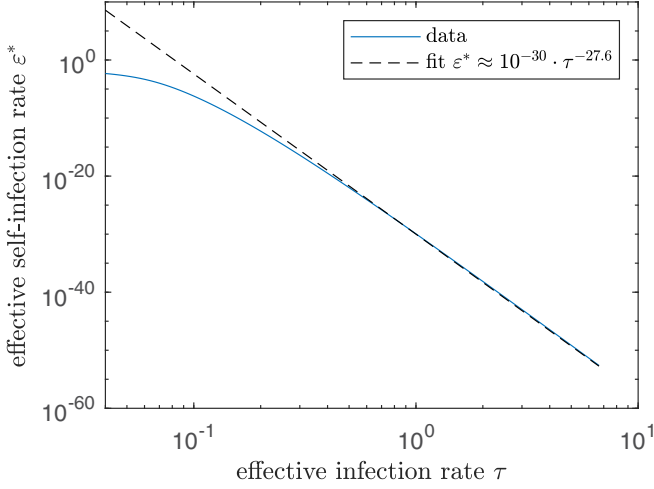


FIG. 15. Illustration of the effective self-infection rate ε^* for which the metastable prevalence y and the steady-state prevalence y_∞ are equal. The power-law tail is observed for $\tau > 0.3 \approx 9\tau_c^{(1)}$ and the results are obtained on a graph with $N = 30$ nodes.

APPENDIX B: EQUAL METASTABLE AND STEADY-STATE PREVALENCE

The time-dependent behavior of the ε -SIS process, which is illustrated in Fig. 2, shows that the final steady-state prevalence y_∞ can be lower or higher than the prevalence y in the metastable state. For a given network size N and effective infection rate τ , we believe that there always exists some $\varepsilon^* > 0$ for which the prevalence in the metastable state and the steady-state prevalence y_∞ are equal. We numerically determine this self-infection rate ε^* and depict the result in Fig. 15. We only show effective infection rates τ that are larger than the epidemic threshold τ_c , because the metastable state does not exist below the threshold. If the effective infection rate τ is sufficiently large, Fig. 15 depicts a power-law decay with exponent $\alpha = -27.6$.

We find an explanation for this result in Theorem 4 by Van Mieghem [7], which states that the epidemic threshold τ_c for sufficiently small ε^* is bounded by

$$\frac{1}{e} \left(\frac{10^{-s}}{\varepsilon^*(N-1)!} \right)^{\frac{1}{N-1}} < \tau_c < \left(\frac{10^{-s}}{\varepsilon^*(N-1)!} \right)^{\frac{1}{N-1}},$$

where 10^{-s} specifies an agreed fraction of infected nodes that determines whether an outbreak has taken place. Considering that the final steady-state prevalence y_∞ is of order 1, we choose $s = 0$. Naturally, the equation can be rewritten in terms of the effective self-infection rate ε^* :

$$\frac{1}{e^{1-N}(N-1)!} \tau^{1-N} \leq \varepsilon^* \leq \frac{1}{(N-1)!} \tau^{1-N}. \quad (\text{B1})$$

Considering the example in Fig. 15 with $N = 30$ nodes, our estimation (B1) states that

$$10^{-19} \tau^{-29} \leq \varepsilon^* \leq 10^{-31} \tau^{-29}.$$

The estimation is very similar to the fitted function from Fig. 15, but for larger effective self-infection rates ε^* , the approximated solution (B1) starts to deviate.

APPENDIX C: MEAN-FIELD ε -SIS

The well-known N -intertwined mean-field approximation (NIMFA) [16] assumes that any two stochastic variables X and Y are uncorrelated: $E[XY] = E[X]E[Y]$. Applying the mean-field approximation to the ε -SIS process on the complete graph, the governing equations become (Ref. [32], p. 462)

$$\frac{d\mathbf{s}_{\text{MF}}(t)}{dt} = \varepsilon \mathbf{u} - (\delta + \varepsilon) \mathbf{s}_{\text{MF}}(t) + \text{diag}[\mathbf{u} - \mathbf{s}_{\text{MF}}(t)] \tilde{B} \mathbf{s}_{\text{MF}}(t), \quad (\text{C1})$$

where $\mathbf{s}_{\text{MF}}(t) = (s_1(t), \dots, s_N(t))^T$ is the $N \times 1$ viral state vector, $\mathbf{u} = (1, \dots, 1)^T$ is the $N \times 1$ all-ones vector, and $\tilde{B} = \beta(\mathbf{u}\mathbf{u}^T - I)$, where I is the $N \times N$ identity matrix. As an upper bound to Eq. (C1), we consider the ε -NIMFA process with self-loops, thus $\beta_{ii} = \beta > 0$. Furthermore, we rescale time $\tilde{t} = \delta t$, and introducing the effective infection rate $\tau = \beta/\delta$ and the effective self-infection rate $\varepsilon^* = \varepsilon/\delta$, we find, after dropping the tildes,

$$\frac{d\mathbf{s}_{\text{MF}}(t)}{dt} = \varepsilon^* \mathbf{u} - (1 + \varepsilon^*) \mathbf{s}_{\text{MF}}(t) + \text{diag}[\mathbf{u} - \mathbf{s}_{\text{MF}}(t)] B \mathbf{s}_{\text{MF}}(t), \quad (\text{C2})$$

where $B = \tau \mathbf{u}\mathbf{u}^T$. We adopt the approach in [36] to obtain the solution of the ε -SIS process on the complete graph. Since the Markovian ε -SIS process is non-negatively correlated [42] and we introduced self-loops $\beta_{ii} > 0$, the solution of (C2) is a strict upper bound for Markovian ε -SIS dynamics.

Proof of Theorem IV.1. We prove Theorem IV.1 in three steps. First, in Appendix C1, we show that the viral state $\mathbf{s}_{\text{MF}}(t)$ is in a two-dimensional subspace at every time t . More specifically, we show that $\mathbf{s}_{\text{MF}}(t) = c_1(t)\mathbf{z}_1 + c_2(t)\mathbf{z}_2$ for two $N \times 1$ agitation modes $\mathbf{z}_1, \mathbf{z}_2$ and two scalar functions $c_1(t), c_2(t) \in \mathbb{R}$. Second, in Appendix C2, we obtain the closed-form expression for the function $c_1(t)$. Third, given the function $c_1(t)$, we obtain the function $c_2(t)$ in Appendix C3.

1. The viral state is in a two-dimensional subspace

With the definition of the agitation mode \mathbf{z}_1 in (8), we can write the infection rate matrix B as

$$B = \tau N \mathbf{z}_1 \mathbf{z}_1^T.$$

Thus, ε -NIMFA on the complete graph (C2) becomes

$$\begin{aligned} \frac{d\mathbf{s}_{\text{MF}}(t)}{dt} &= \varepsilon^* \sqrt{N} \mathbf{z}_1 - (1 + \varepsilon^*) \mathbf{s}_{\text{MF}}(t) + \text{diag}(\sqrt{N} \mathbf{z}_1 \\ &\quad - \mathbf{s}_{\text{MF}}(t)) \tau N \mathbf{z}_1 \mathbf{z}_1^T \mathbf{s}_{\text{MF}}(t). \end{aligned}$$

Suppose that (7) holds at time t . Then, we obtain that

$$\begin{aligned} \frac{d\mathbf{s}_{\text{MF}}(t)}{dt} &= \varepsilon^* \sqrt{N} \mathbf{z}_1 - (1 + \varepsilon^*) c_1(t) \mathbf{z}_1 - (1 + \varepsilon^*) c_2(t) \mathbf{z}_2 \\ &\quad + \text{diag}[(\sqrt{N} - c_1(t)) \mathbf{z}_1 - c_2(t) \mathbf{z}_2] \tau N \mathbf{z}_1 \mathbf{z}_1^T [c_1(t) \mathbf{z}_1 \\ &\quad + c_2(t) \mathbf{z}_2]. \end{aligned}$$

Since $\mathbf{z}_1^T \mathbf{z}_1 = 1$ and $\mathbf{z}_1^T \mathbf{z}_2 = 0$, it follows that

$$\begin{aligned} \frac{d\mathbf{s}_{\text{MF}}(t)}{dt} &= (\varepsilon^* \sqrt{N} - (1 + \varepsilon^*)c_1(t))\mathbf{z}_1 - (1 + \varepsilon^*)c_2(t)\mathbf{z}_2 \\ &\quad + \tau N c_1(t) \text{diag}[(\sqrt{N} - c_1(t))\mathbf{z}_1 - c_2(t)\mathbf{z}_2]\mathbf{z}_1, \end{aligned}$$

which is equivalent to

$$\begin{aligned} \frac{d\mathbf{s}_{\text{MF}}(t)}{dt} &= (\varepsilon^* \sqrt{N} - (1 + \varepsilon^*)c_1(t))\mathbf{z}_1 - (1 + \varepsilon^*)c_2(t)\mathbf{z}_2 \\ &\quad + \tau N (\sqrt{N}c_1(t) - c_1^2(t)) \text{diag}(\mathbf{z}_1)\mathbf{z}_1 \\ &\quad - \tau N c_1(t)c_2(t) \text{diag}(\mathbf{z}_2)\mathbf{z}_1. \end{aligned}$$

From the definition of the agitation mode \mathbf{z}_1 in (8), we obtain that $\text{diag}(\mathbf{z}_1)\mathbf{z}_1 = \mathbf{z}_1/\sqrt{N}$ and $\text{diag}(\mathbf{z}_2)\mathbf{z}_1 = \mathbf{z}_2/\sqrt{N}$. Thus, we arrive at

$$\begin{aligned} \frac{d\mathbf{s}_{\text{MF}}(t)}{dt} &= (\varepsilon^* \sqrt{N} - (1 + \varepsilon^*)c_1(t))\mathbf{z}_1 - (1 + \varepsilon^*)c_2(t)\mathbf{z}_2 \\ &\quad + \tau \sqrt{N} (\sqrt{N}c_1(t) - c_1^2(t))\mathbf{z}_1 - \tau \sqrt{N} c_1(t)c_2(t)\mathbf{z}_2, \end{aligned}$$

which simplifies to

$$\begin{aligned} \frac{d\mathbf{s}_{\text{MF}}(t)}{dt} &= (\varepsilon^* \sqrt{N} + (\tau N - 1 - \varepsilon^*)c_1(t) - \tau \sqrt{N}c_1^2(t))\mathbf{z}_1 \\ &\quad - (1 + \varepsilon^* + \tau \sqrt{N}c_1(t))c_2(t)\mathbf{z}_2. \end{aligned} \tag{C3}$$

Hence, the $N \times 1$ viral state vector $\mathbf{s}_{\text{MF}}(t)$ is equal to the linear combination (7) of only two agitation modes $\mathbf{z}_1, \mathbf{z}_2$ at every time t . Thus, solving ε -NIMFA on the complete graph simplifies to obtaining a closed-form expression for the functions $c_1(t)$ and $c_2(t)$.

2. First agitation mode

Since

$$\frac{dc_l(t)}{dt} = \mathbf{z}_l^T \frac{d\mathbf{s}_{\text{MF}}(t)}{dt} \tag{C4}$$

for both $l = 1, 2$, we obtain for the scalar function $c_1(t)$ from (C3) that

$$\frac{dc_1(t)}{dt} = \varepsilon^* \sqrt{N} + (\tau N - 1 - \varepsilon^*)c_1(t) - \tau \sqrt{N}c_1^2(t). \tag{C5}$$

The differential equation (C5) is separable,

$$\frac{dc_1(t)}{-\tau \sqrt{N}c_1^2(t) + (\tau N - 1 - \varepsilon^*)c_1(t) + \varepsilon^* \sqrt{N}} = dt.$$

Hence, it follows that

$$\frac{dc_1(t)}{c_1^2(t) + \mu_1 c_1(t) - \mu_2} = -\tau \sqrt{N} dt \tag{C6}$$

with the constants

$$\mu_1 = \frac{1 + \varepsilon^* - \tau N}{\tau \sqrt{N}} \tag{C7}$$

and

$$\mu_2 = \frac{\varepsilon^*}{\tau}. \tag{C8}$$

We obtain from (C6) that

$$\int \frac{dc_1(t)}{c_1^2(t) + \mu_1 c_1(t) - \mu_2} = -\tau \sqrt{N} t + K(c_1(0))$$

for some constant $K(c_1(0)) \in \mathbb{R}$. By integration, it follows that

$$\frac{2}{\sqrt{-4\mu_2 - \mu_1^2}} \tan^{-1} \left(\frac{\mu_1 + 2c_1(t)}{\sqrt{-4\mu_2 - \mu_1^2}} \right) = -\tau \sqrt{N} t + K(c_1(0)),$$

which yields that

$$\frac{\mu_1 + 2c_1(t)}{\sqrt{-4\mu_2 - \mu_1^2}} = \tan \left(\frac{1}{2} \sqrt{-4\mu_2 - \mu_1^2} (-\tau \sqrt{N} t + K(c_1(0))) \right).$$

We isolate for $c_1(t)$ and arrive at

$$c_1(t) = -\frac{1}{2}\mu_1 + \frac{1}{2}\sqrt{-4\mu_2 - \mu_1^2} \tan \left(\frac{1}{2}\sqrt{-4\mu_2 - \mu_1^2} (-\tau \sqrt{N} t + K(c_1(0))) \right).$$

With the imaginary unit $i = \sqrt{-1}$, it follows that

$$c_1(t) = -\frac{1}{2}\mu_1 + \frac{1}{2}i \sqrt{\mu_1^2 + 4\mu_2} \tan \left(\frac{1}{2}i \sqrt{\mu_1^2 + 4\mu_2} (-\tau \sqrt{N} t + K(c_1(0))) \right).$$

Finally, with the relation $i \tan(ix) = -\tanh(x)$ of the tangent and hyperbolic tangent and with $-\tanh(x) = \tanh(-x)$ for all $x \in \mathbb{R}$, we arrive at

$$c_1(t) = -\frac{1}{2}\mu_1 + \frac{1}{2}\sqrt{\mu_1^2 + 4\mu_2} \tanh \left(\frac{1}{2}\sqrt{\mu_1^2 + 4\mu_2} (\tau \sqrt{N} t - K(c_1(0))) \right). \tag{C9}$$

To further simplify (C9), we obtain with the definition of the constants μ_1 and μ_2 in (C7) and (C8) that

$$\sqrt{\mu_1^2 + 4\mu_2} = \sqrt{\frac{(1 + \varepsilon^* - \tau N)^2}{\tau^2 N} + 4\frac{\varepsilon^*}{\tau}},$$

which simplifies to

$$\sqrt{\mu_1^2 + 4\mu_2} = \frac{1}{\tau\sqrt{N}} w_{\varepsilon^*}, \quad (\text{C10})$$

where we define the *viral slope* w_{ε^*} for ε -NIMFA as

$$w_{\varepsilon^*} = \sqrt{(1 + \varepsilon^* - \tau N)^2 + 4\varepsilon^* \tau N}.$$

If $\varepsilon^* = 0$, then the viral slope w_{ε^*} equals $w_{\varepsilon^*} = |w|$, where w is the viral slope of the NIMFA model, defined in [43]. With (C10) and the definition of μ_1 in (C7), the function $c_1(t)$ in (C9) becomes

$$c_1(t) = \frac{1}{2} \frac{\tau N - 1 - \varepsilon^*}{\tau\sqrt{N}} + \frac{1}{2} \frac{1}{\tau\sqrt{N}} w_{\varepsilon^*} \tanh\left(\frac{w_{\varepsilon^*}}{2} t + \Upsilon_{1,\varepsilon^*}(c_1(0))\right)$$

with the constant $\Upsilon_{1,\varepsilon^*}(c_1(0)) = -\frac{1}{2} \frac{1}{\tau\sqrt{N}} w_{\varepsilon^*} K(c_1(0))$. Thus, it holds that

$$c_1(t) = \frac{1}{2\tau\sqrt{N}} \left[\tau N - 1 - \varepsilon^* + w_{\varepsilon^*} \tanh\left(\frac{w_{\varepsilon^*}}{2} t + \Upsilon_{1,\varepsilon^*}(c_1(0))\right) \right]. \quad (\text{C11})$$

The initial condition of the projection $c_1(t)$ is given by $c_1(0) = \mathbf{z}_1^T \mathbf{s}_{\text{MF}}(0)$, which yields for the constant $\Upsilon_{\varepsilon^*}(c_1(0))$ that

$$\Upsilon_{1,\varepsilon^*}(c_1(0)) = \operatorname{arctanh}\left(\frac{1}{w_{\varepsilon^*}} (2\tau\sqrt{N} \mathbf{z}_1^T \mathbf{s}_{\text{MF}}(0) - \tau N + 1 + \varepsilon^*)\right).$$

3. Second agitation mode

From (C4) for $l = 2$, it follows with (C3) that the scalar function $c_2(t)$ obeys

$$\frac{dc_2(t)}{dt} = -(1 + \varepsilon^* + \tau\sqrt{N}c_1(t))c_2(t). \quad (\text{C12})$$

The closed-form expression for the function $c_1(t)$ is given in (C11), and the differential equation (C12) becomes

$$\frac{dc_2(t)}{dt} = -(1 + \varepsilon^*)c_2(t) - \frac{1}{2} \left[\tau N - 1 - \varepsilon^* + w_{\varepsilon^*} \tanh\left(\frac{w_{\varepsilon^*}}{2} t + \Upsilon_{1,\varepsilon^*}(c_1(0))\right) \right] c_2(t) \quad (\text{C13})$$

$$= -\frac{1 + \varepsilon^* + \tau N}{2} c_2(t) - \frac{w_{\varepsilon^*}}{2} \tanh\left(\frac{w_{\varepsilon^*}}{2} t + \Upsilon_{1,\varepsilon^*}(c_1(0))\right) c_2(t). \quad (\text{C14})$$

The remaining steps are similar to Ref. [36] (Proof of Theorem 4). Since

$$\frac{d \ln(c_2(t))}{dt} = \frac{1}{c_2(t)} \frac{dc_2(t)}{dt},$$

we obtain that

$$\frac{d \ln(c_2(t))}{dt} = -\frac{1 + \varepsilon^* + \tau N}{2} - \frac{w_{\varepsilon^*}}{2} \tanh\left(\frac{w_{\varepsilon^*}}{2} t + \Upsilon_{1,\varepsilon^*}(c_1(0))\right). \quad (\text{C15})$$

The integral of the hyperbolic tangent equals [44]

$$\int \tanh(\xi) d\xi = \ln(\cosh(\xi)) + C$$

for an arbitrary constant $C \in \mathbb{R}$, where $\cosh(\xi)$ denotes the hyperbolic cosine. Hence, we obtain with the chain rule from (C15) that

$$\ln(c_2(t)) = -\frac{1 + \varepsilon^* + \tau N}{2} t - \frac{w_{\varepsilon^*}}{2} \frac{2}{w_{\varepsilon^*}} \ln\left(\cosh\left(\frac{w_{\varepsilon^*}}{2} t + \Upsilon_{1,\varepsilon^*}(c_1(0))\right)\right) + C$$

for some constant $C \in \mathbb{R}$. Thus, exponentiation yields that the function $c_2(t)$ equals

$$\begin{aligned} c_2(t) &= \exp(C) \exp\left(-\frac{1 + \varepsilon^* + \tau N}{2} t\right) \left[\cosh\left(\frac{w_{\varepsilon^*}}{2} t + \Upsilon_{1,\varepsilon^*}(c_1(0))\right) \right]^{-1} \\ &= \Upsilon_{2,\varepsilon^*}(c_2(0)) \exp\left(-\frac{1 + \varepsilon^* + \tau N}{2} t\right) \operatorname{sech}\left(\frac{w_{\varepsilon^*}}{2} t + \Upsilon_{1,\varepsilon^*}(c_1(0))\right), \end{aligned}$$

where we denote the hyperbolic secant by $\operatorname{sech}(\xi) = \cosh(\xi)^{-1}$. The constant $\Upsilon_{2,\varepsilon^*}(c_2(0))$ follows from the initial condition $c_2(0) = \mathbf{z}_2^T \mathbf{s}_{\text{MF}}(0)$ as

$$\Upsilon_{2,\varepsilon^*}(c_2(0)) = \mathbf{z}_2^T \mathbf{s}_{\text{MF}}(0) \cosh(\Upsilon_{1,\varepsilon^*}(c_1(0))). \quad (\text{C16})$$

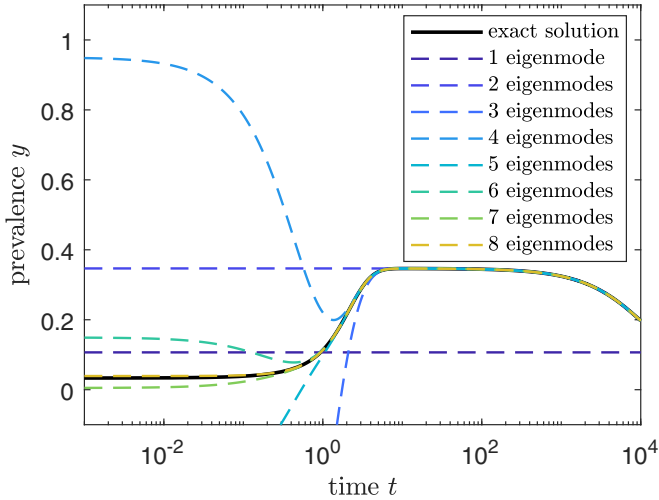


FIG. 16. The time-varying prevalence $y(t)$ for the complete graph with $N = 30$ nodes, effective infection rate $\tau = 2.5\tau_c^{(1)}$, and effective self-infection rate $\varepsilon^* = 10^{-6}$. The solid line indicates the solution (5), and the dashed lines show the approximation (D1) for various values of m .

APPENDIX D: EIGENVALUE TRUNCATION OF THE ε -SIS PROCESS

If the metastable state exists, Fig. 2 depicts roughly three regimes for the time-varying prevalence: (I) initial phase, (II) metastable behavior, and (III) convergence to the steady state. Since the behavior is rather limited, we expect that the time-dependent dynamics of the ε -SIS process can be accurately approximated. Apart from the largest eigenvalue $\xi_1 = 0$ and the second-largest eigenvalue ξ_2 , the majority of the eigenvalues are largely clustered. The $(N + 1)$ -sized linear process (1) can perhaps be approximated accurately with only $m \ll (N + 1)$ eigenvalues and eigenvectors. This methodology has been applied successfully for the mean-field SIS model around the epidemic threshold [43], but to the best of our knowledge, no results have been obtained for the Markovian SIS process.

We approximate the solution (5) by considering only the m largest eigenvalues and corresponding eigenvectors:

$$\tilde{\mathbf{s}}(t) = \sum_{k=1}^m c_k e^{\xi_k t} \mathbf{w}_k, \quad (\text{D1})$$

where $c_k = \mathbf{v}_k^T \mathbf{s}(0)$. Approximating the exact solution (5) by the approximation (D1) introduces an error,

$$e(t) = \|\mathbf{s}(t) - \tilde{\mathbf{s}}(t)\| = \left\| \sum_{k=m+1}^{N+1} c_k e^{\xi_k t} \mathbf{w}_k \right\| \leq \sum_{k=m+1}^{N+1} e^{\xi_k t} \|c_k \mathbf{w}_k\|,$$

where $\|\cdot\|$ denotes a vector norm and we used the vector inequality $\|\mathbf{a} + \mathbf{b}\| \leq \|\mathbf{a}\| + \|\mathbf{b}\|$. Further, since eigenvectors are normalized with norm 1,

$$e(t) \leq \sum_{k=m+1}^{N+1} e^{\xi_k t} \|c_k \mathbf{w}_k\| < e^{\xi_{m+1} t} \sum_{k=m+1}^{N+1} |c_k|.$$

Thus the error scales as $e(t) = O(e^{\xi_{m+1} t})$. Figure 16 shows the solution (5) and the approximation (D1) for various choices

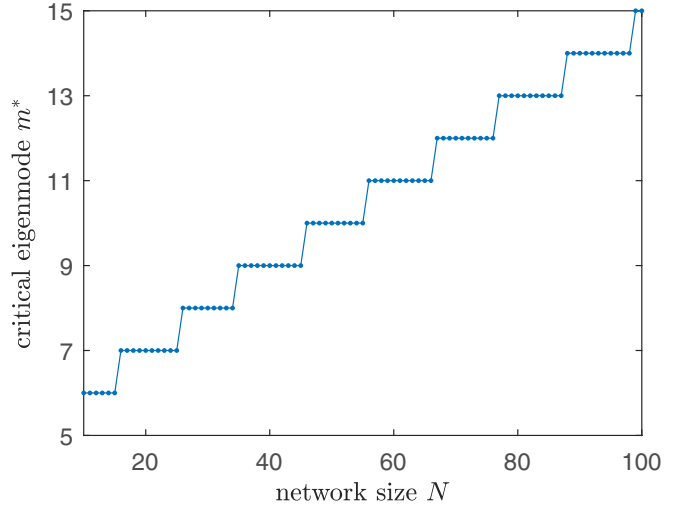


FIG. 17. The relation between the critical number of eigenvalues m^* and the number of nodes N in the graph. The critical number m^* is defined as the smallest integer m for which the initial prevalence $\tilde{y}(0)$ of the approximated solution (D1) differs at most 10^{-3} from the initial prevalence $y(0)$ of the exact solution (1).

of m . The original solution (5) is recovered accurately using only $m = 8$ from the total of 31 eigenvalues.

We define the critical number of eigenvalues m^* as the smallest m for which $|y(0) - \tilde{y}(0)| \leq 10^{-3}$, where $y(0)$ and $\tilde{y}(0)$ describe the initial prevalence of the exact solution (5) and approximated solution (D1), respectively. The critical number m^* is an integer between 1 and $N + 1$. Figure 17 shows an apparent linear relationship between the critical number m^* and the network size N . Even though an accurate approximation is possible, the number of required eigenvalues grows linearly with the network size N , effectively rendering the approximation method infeasible for large networks. This contrasts results for the mean-field ε -SIS process with arbitrary initial conditions but homogeneous parameters, where the number of required equations reduces to only two (see Appendix C).

APPENDIX E: EIGENVALUE APPROXIMATIONS AND BOUNDS

This Appendix contains all proofs for the eigenvalues ξ_k of the transition matrix P in Eq. (2) in several parameters limits. Most proofs use the symmetric transition matrix \tilde{P} , which is derived in Appendix A. We start by presenting Theorem E.1.

Theorem E.1 (based on Ref. [45], pp. 366–372, and Ref. [46], pp. 303–321). Given a Hermitian matrix $P = A + \alpha B$, where A and B are Hermitian matrices and α is a small parameter, such that the element a_{ij} is strictly larger than b_{ij} for all α and all $1 \leq i, j \leq N$. We assume that the eigenvalues $\xi_k^{(0)}$ and eigenvectors $\mathbf{x}_k^{(0)}$ of the unperturbed matrix A can be computed easily.

(a) If an eigenvalue $\xi_k^{(0)}$ of A is *simple*, then the eigenvalue ξ_k of P is up to fourth order

$$\begin{aligned} \xi_k &= \xi_k^{(0)} + \alpha W_{kk} + \alpha^2 \sum_{\substack{l=1 \\ l \neq k}}^N \frac{|W_{lk}|^2}{\xi_k^{(0)} - \xi_l^{(0)}} \\ &+ \alpha^3 \sum_{\substack{l=1 \\ l \neq k}}^N (W_{ll} - W_{kk}) \left(\frac{W_{kl}}{\xi_k^{(0)} - \xi_l^{(0)}} \right)^2 \\ &+ \alpha^3 \sum_{\substack{l=1 \\ l \neq k}}^N \sum_{\substack{m=1 \\ m \neq k}}^N \frac{W_{kl} W_{lm} W_{mk}}{(\xi_k^{(0)} - \xi_l^{(0)})(\xi_k^{(0)} - \xi_m^{(0)})} + O(\alpha^4), \end{aligned}$$

where $W_{ij} = (\mathbf{x}_i^{(0)})^T B \mathbf{x}_j^{(0)}$.

(b) If an eigenvalue $\xi_k^{(0)}$ of A is *twofold single degenerate*,⁵ then the eigenvalue ξ_k of P is up to third order

$$\xi_k = \xi_k^{(0)} + \alpha \xi_k^{(1)} + \alpha^2 \sum_{\substack{l=1 \\ l \neq k_1 \\ l \neq k_2}}^N \frac{|W'_{lk}|^2}{\xi_k^{(0)} - \xi_l^{(0)}} + O(\alpha^3),$$

where the eigenvalues $\xi_k^{(1)}$ are determined from the eigenvalue equation

$$\begin{pmatrix} W_{k_1, k_1} & W_{k_1, k_2} \\ W_{k_2, k_1} & W_{k_2, k_2} \end{pmatrix} \begin{pmatrix} \alpha_k \\ \beta_k \end{pmatrix} = \xi_k^{(1)} \begin{pmatrix} \alpha_k \\ \beta_k \end{pmatrix}, \quad (\text{E1})$$

where $W_{ij} = (\mathbf{x}_i^{(0)})^T B \mathbf{x}_j^{(0)}$. The indices k_1 and k_2 correspond to the degenerate eigenvalues $\xi_k^{(0)} = \xi_{k_1}^{(0)} = \xi_{k_2}^{(0)}$. The corrected zero-order eigenvectors are $\mathbf{x}_k^{(0)} = \alpha_{k_1} \mathbf{x}_{k_1}^{(0)} + \beta_{k_2} \mathbf{x}_{k_2}^{(0)}$. The second-order correction term requires the W' matrix, which has elements $W'_{ij} = (\mathbf{x}_i^{(0)})^T B \mathbf{x}_j^{(0)}$.

(c) If an eigenvalue $\xi_k^{(0)}$ of A is *twofold double degenerate*,⁶ then the eigenvalue ξ_k of P is up to third order

$$\begin{aligned} \xi_k &= \xi_k^{(0)} + \frac{\alpha}{2} (W_{k_1, k_1} + W_{k_2, k_2} \pm \sqrt{(W_{k_1, k_1} - W_{k_2, k_2})^2 + 4W_{k_1, k_2} W_{k_2, k_1}}) \\ &+ \frac{\alpha^2}{2} (M_{k_1, k_1} + M_{k_2, k_2} \pm \sqrt{(M_{k_1, k_1} - M_{k_2, k_2})^2 + 4M_{k_1, k_2} M_{k_2, k_1}}) + O(\alpha^3), \end{aligned}$$

where $W_{ij} = (\mathbf{x}_i^{(0)})^T B \mathbf{x}_j^{(0)}$ and

$$M_{ij} = \sum_{\substack{m=1 \\ m \neq i \\ m \neq j}}^N \frac{W_{i,m} W_{m,j}}{\xi_i^{(0)} - \xi_m^{(0)}}.$$

Sketch of the proof. Instead of providing a proof, we sketch the idea of the proof here. An actual proof can be based on [45] and/or [46].

The primary goal of this theorem is to approximate the eigenvalues of a matrix P , for which exact computations are generally infeasible. Defining a small variable α , we split up the Hermitian (or here, symmetric) matrix P into $P = A + \alpha B$, where A is a diagonal matrix and B contains the remaining, symmetric terms. We emphasize that both A and B may contain functions of α , as long as the element a_{ij} is larger than b_{ij} for all i, j in the limit $\alpha \rightarrow 0$. The division of P into A and B is generally not unique, but the number of choices is heavily restricted by the small parameter α .

If the eigenvalue ξ_k of the matrix A is nondegenerate, one can perform an ordinary eigenvalue expansion that can be found in any textbook covering perturbation expansions of linear operators [part (a)]. Some eigenvalues may appear

multiple times in the spectrum of A , which complicates the analysis. In our case, each eigenvalue exists at most twice, thus we confine ourselves to twofold degeneracy. The procedure can be easily generalized to n -fold degeneracy.

If the eigenvalues $\xi_k^{(0)}$ are twofold-degenerate, the corresponding eigenvectors are not determined up to a scalar value, but are only known to be in the span of two vectors. We can choose the eigenvectors freely, as long as they belong to the span and are orthonormal to each other. If the eigenvalues are distinct at the first order, that is, the degeneracy is lifted at the first order [part (b)], we can determine the zeroth-order eigenvectors and use that basis as if we would perform a regular expansion as in part (a), with the exception that the summation over all terms excludes both the current index k as well as the index k' corresponding to the same zero-order eigenvalue $\xi_k^{(0)} = \xi_{k'}^{(0)}$ and that we use the zeroth-order eigenvectors $\mathbf{x}_k^{(0)}$ instead of the original $\mathbf{x}_k^{(0)}$.

If the first-order correction of the eigenvalue still maintains the degeneracy, the second-order correction of the eigenvalues must be computed [part (c)]. As before, if the eigenvalues are no longer degenerate after adding the second-order correction, the zeroth-order eigenvectors can be determined. The procedure can be repeated up to higher orders, which is outside of the scope of this theorem.

1. The limit $\epsilon^* \rightarrow \infty$

Proof. The symmetric transition matrix \tilde{P} from Eq. (A1) can be rewritten as

$$\tilde{P} = \tilde{A} + \tilde{B},$$

⁵An eigenvalue ξ of some matrix A is *twofold single degenerate* if the eigenvalue ξ appears twice in the spectrum of A and is no longer degenerate after adding the first correction term.

⁶An eigenvalue ξ of some matrix A is *twofold double degenerate* if the eigenvalue ξ appears twice in the spectrum of A and is no longer degenerate after adding the second-order correction term.

where \tilde{A} is a diagonal matrix with elements

$$\tilde{A}_{kk} = -\varepsilon^*(N - k) \quad \text{for } k = 0, 1, \dots, N$$

and \tilde{B} is a symmetric, tridiagonal matrix with elements

$$\begin{aligned} \tilde{B}_{kk} &= -\tau k(N - k) - k, \\ \tilde{B}_{k-1,k} &= \sqrt{k(N - k + 1)[(k - 1)\tau + \varepsilon^*]}. \end{aligned}$$

We define the small parameter $\alpha = \frac{1}{\sqrt{\varepsilon^*}}$ (which is small, because $\varepsilon^* \rightarrow \infty$), such that $\alpha^2 \tilde{P} = A + \alpha B$, where we defined $A = \alpha^2 \tilde{A}$ and $B = \alpha \tilde{B}$. The matrix A is a diagonal matrix with

elements

$$A_{kk} = -(N - k)$$

and the matrix B is then tridiagonal with elements

$$\begin{aligned} B_{kk} &= -\alpha k[\tau(N - k) + 1], \\ B_{k-1,k} &= \sqrt{k(N - k + 1)[(k - 1)\tau\alpha^2 + 1]}. \end{aligned}$$

The eigenvalues of A are simply $a_k = -(N - k)$ for $k = 0, 1, \dots, N$ and the corresponding eigenvector $\mathbf{x}_k = \mathbf{e}_k$, where \mathbf{e}_k is the $(N + 1) \times 1$ all-zeros vector, except at entry k , where it is 1. Since $\mathbf{x}_k = \mathbf{e}_k$, we immediately find that $W_{lk} = \mathbf{x}_l^T B \mathbf{x}_k = B_{kl}$. In the same manner, we find $a_k - a_l = k - l$. Given the uniqueness of the eigenvalues a_k , we follow part (a) of Theorem E.1 to find

$$\alpha^2 \xi_k = -(N - k) + \alpha B_{kk} + \alpha^2 \sum_{\substack{l=1 \\ l \neq k}}^N \frac{(B_{kl})^2}{k - l} + \alpha^3 \sum_{\substack{l=1 \\ l \neq k}}^N (B_{ll} - B_{kk}) \left(\frac{B_{lk}}{k - l} \right)^2 + \alpha^3 \sum_{\substack{l=1 \\ l \neq k}}^N \sum_{\substack{m=1 \\ m \neq k \\ m \neq l}}^N \frac{B_{lk} B_{ml} B_{km}}{(k - l)(k - m)} + O(\alpha^4).$$

The value B_{kl} is only nonzero if $l \in \{k - 1, k, k + 1\}$. We conclude that $B_{lk} B_{ml} B_{km} = 0$ if $k \neq l \neq m$. Thus

$$\alpha^2 \xi_k = -(N - k) + \alpha B_{kk} + \alpha^2 \sum_{\substack{l=1 \\ l \neq k}}^N \frac{(B_{kl})^2}{k - l} + \alpha^3 \sum_{\substack{l=1 \\ l \neq k}}^N (B_{ll} - B_{kk}) \left(\frac{B_{lk}}{k - l} \right)^2 + O(\alpha^4).$$

The α^2 -term can be worked out as follows:

$$\begin{aligned} \sum_{\substack{l=1 \\ l \neq k}}^N \frac{(B_{kl})^2}{k - l} &= \left(\frac{B_{k,k-1}^2}{k - (k - 1)} + \frac{B_{k,k+1}^2}{k - (k + 1)} \right) \\ &= [\tau\alpha^2(k - 1) + 1](N - k + 1)k - (\tau\alpha^2 k + 1)(N - k)(k + 1) \\ &= \tau\alpha^2[(k - 1)(N - k + 1)k - k(N - k)(k + 1)] + [(N - k + 1)k - (N - k)(k + 1)] \\ &= \tau\alpha^2 k(3k - 2N - 1) + (2k - N). \end{aligned}$$

The α^3 -term can be worked out as follows:

$$\begin{aligned} \sum_{\substack{l=1 \\ l \neq k}}^N (B_{ll} - B_{kk}) \left(\frac{B_{lk}}{k - l} \right)^2 &= \alpha \left((2\tau k - \tau N - \tau - 1) \frac{B_{k,k-1}^2}{[k - (k - 1)]^2} + (2\tau k - \tau N + \tau - 1) \frac{B_{k,k+1}^2}{[k - (k + 1)]^2} \right) \\ &= \alpha(2\tau k - \tau N - \tau - 1)[\tau\alpha^2(k - 1) + 1](N - k + 1)k \\ &\quad + \alpha(2\tau k - \tau N + \tau - 1)(\tau\alpha^2 k + 1)(N - k)(k + 1) \\ &= -8\alpha^3 k^3 \tau^2 + 3\alpha^3 k^2 \tau^2 + 3\alpha^3 k^2 \tau - 6\alpha k^2 \tau + 9\alpha^3 k^2 N \tau^2 - \alpha^3 k \tau^2 - \alpha^3 k \tau \\ &\quad + 2\alpha k - 2\alpha^3 k N^2 \tau^2 - \alpha^3 k N \tau^2 - 2\alpha^3 k N \tau + 6\alpha k N \tau - \alpha N^2 \tau + \alpha N \tau - \alpha N \\ &= -6\alpha k^2 \tau + 2\alpha k + 6\alpha k N \tau - \alpha N^2 \tau + \alpha N \tau - \alpha N + O(\alpha^3). \end{aligned}$$

Assembling the results, we find

$$\begin{aligned} \alpha^2 \xi_k &= -(N - k) + \alpha^2[-\tau k(N - k) - k] + \alpha^2(\tau\alpha^2 k(3k - 2N - 1) + (2k - N)) \\ &\quad + \alpha^4(-6k^2 \tau + 2k + 6k N \tau - N^2 \tau + N \tau - N) + O(\alpha^4). \end{aligned}$$

Using $\alpha^2 = 1/\varepsilon^*$, we find

$$\begin{aligned} \xi_k &= -\varepsilon^*(N - k) - [\tau k(N - k) + k] + \left(\frac{1}{\varepsilon^*} \tau k(3k - 2N - 1) + (2k - N) \right) \\ &\quad + \frac{1}{\varepsilon^*} (-6k^2\tau + 2k + 6kN\tau - N^2\tau + N\tau - N) + O\left(\frac{1}{\varepsilon^*}\right). \end{aligned}$$

The index $k = 0, 1, \dots, N$ can be transformed so as to make sure that the eigenvalues ξ_k are descending: $0 = \xi_1 > \xi_2 > \dots > \xi_{N+1}$. We define the index $\hat{k} = N - k + 1$, which takes values in $\hat{k} = 1, 2, \dots, N + 1$ such that we recover

$$\begin{aligned} \xi_{\hat{k}} &= -(\hat{k} - 1)\varepsilon^* - (\hat{k} - 1)[\tau(N + 1 - \hat{k}) + 1] \\ &\quad + (\tau(2N + 2\hat{k}N - 2 - 5\hat{k} - 3\hat{k}^2) + N - 2 - 2\hat{k})\frac{1}{\varepsilon^*} + O\left(\frac{1}{\varepsilon^*}\right), \end{aligned}$$

which concludes our proof. Presumably the $O(\alpha^4)$ -terms will bring additional terms for the $O(\frac{1}{\varepsilon^*})$ -term in the final solution, thus our estimate is only correct until $O(\frac{1}{\varepsilon^*})$.

2. The limit $\tau \rightarrow \infty$

If the effective infection rate τ tends to infinity, then the dynamics of the ε -SIS process simplifies to an SI process. Metastability cannot be observed in the SI process, because the number of infected nodes only increases, until all nodes are infected. The exact time-dependent solution of the continuous-time Markovian SI process on any fixed graph with heterogeneous infection rates is given in [47].

Proof. The symmetric transition matrix \tilde{P} from Eq. (A1) can be rewritten as

$$\tilde{P} = \tilde{A} + \tilde{B},$$

where \tilde{A} is a diagonal matrix with elements

$$\tilde{A}_{kk} = -\tau k(N - k) \quad \text{for } k = 0, 1, \dots, N$$

and \tilde{B} is a symmetric, tridiagonal matrix with elements

$$\begin{aligned} \tilde{B}_{kk} &= -\varepsilon^*(N - k) - k, \\ \tilde{B}_{k-1,k} &= \sqrt{k(N - k + 1)[(k - 1)\tau + \varepsilon^*]}. \end{aligned}$$

We define the small parameter $\alpha = \frac{1}{\sqrt{\tau}}$ (which is small, because $\tau \rightarrow \infty$), such that $\alpha^2 \tilde{P} = A + \alpha B$, where we defined $A = \alpha^2 \tilde{A}$ and $B = \alpha \tilde{B}$. The matrix A is then diagonal with elements

$$A_{kk} = -k(N - k)$$

and the matrix B is then tridiagonal with elements

$$\begin{aligned} B_{kk} &= -\alpha(\varepsilon^*(N - k) + k), \\ B_{k-1,k} &= \sqrt{k(N - k + 1)(k - 1 + \varepsilon^*\alpha^2)}. \end{aligned}$$

The eigenvalues of A are simply $a_k = -k(N - k)$ for $k = 0, 1, \dots, N$ and the corresponding eigenvector $\mathbf{x}_k = \mathbf{e}_k$, where \mathbf{e}_k is the $(N + 1) \times 1$ all-zeros vector, except at entry k where it is 1. We distinguish between networks with even and odd sizes and treat the case $\varepsilon^* = 1$ with special care.

a. Case 1: Even size N

Consider a graph with an even number of nodes N . Then the matrix A has one simple eigenvalue a_k with index $k = N/2$. The remaining eigenvalues are twofold-degenerate. Let a_k and a_{N-k} be a pair of degenerate eigenvalues. Then the eigenvalue equation is according to part (b) from Theorem E.1,

$$\begin{pmatrix} B_{k,k} & B_{k,N-k} \\ B_{N-k,k} & B_{N-k,N-k} \end{pmatrix} \begin{pmatrix} \alpha_k \\ \beta_k \end{pmatrix} = \xi_k^{(1)} \begin{pmatrix} \alpha_k \\ \beta_k \end{pmatrix}. \quad (\text{E2})$$

Since the number of nodes N is even, we know that $B_{k,N-k} = B_{N-k,k} = 0$ for all $k \neq N/2$. Thus the eigenvalue correction equals

$$\begin{aligned} \xi_k^{(1)} &= B_{k,k} = -\alpha(\varepsilon^*(N - k) + k), \\ \xi_{N-k}^{(1)} &= B_{N-k,N-k} = -\alpha(\varepsilon^*k + (N - k)), \end{aligned}$$

which are different for all $k \neq \frac{N}{2}$ and all even network sizes N , except when $\varepsilon^* = 1$. If $\varepsilon^* \neq 1$, the eigenvectors $(\alpha_k \beta_k)^T$ equal the elementary vectors \mathbf{e}_k , which implies⁷ that part (a) from Theorem E.1 can be used instead of part (b).

Applying part (a) from Theorem E.1, we find

$$\begin{aligned} \alpha^2 \xi_k &= a_k + \alpha B_{kk} + \alpha^2 \sum_{\substack{l=1 \\ l \neq k}}^N \frac{(B_{lk})^2}{a_k - a_l} + O(\alpha^3) \\ &= -k(N - k) - \alpha^2(\varepsilon^*(N - k) + k) + \alpha^2 \left(\frac{(B_{k-1,k})^2}{a_k - a_{k-1}} + \frac{(B_{k+1,k})^2}{a_k - a_{k+1}} \right) + O(\alpha^3) \end{aligned}$$

⁷Please consult the sketch of the proof of Theorem E.1 for the complete reasoning.

$$\begin{aligned} &= -k(N - k) - \alpha^2(\varepsilon^*(N - k) + k) + \alpha^2\left(\frac{k(N - k + 1)(k - 1 + \varepsilon^*\alpha^2)}{2k - N - 1} + \frac{(k + 1)(N - k)(k + \varepsilon^*\alpha^2)}{N - 1 - 2k}\right) + O(\alpha^3) \\ &= -k(N - k) + \alpha^2\left(-\varepsilon^*(N - k) + \frac{k(N + 1)(N - k)}{(2k - N - 1)(2k - N + 1)}\right) + O(\alpha^3). \end{aligned}$$

Using $\alpha^2 = \frac{1}{\tau}$, we find the following relationship for the eigenvalues:

$$\xi_k = -\tau k(N - k) + \left(-\varepsilon^*(N - k) + \frac{k(N + 1)(N - k)}{(2k - N - 1)(2k - N + 1)}\right) + O\left(\frac{1}{\sqrt{\tau}}\right). \tag{E3}$$

For $k = \frac{N}{2}$, we simply find

$$\xi_{N/2} = -\tau \frac{N^2}{4} - \frac{N}{2}\left(\varepsilon^* + \frac{N}{2}(N + 1)\right) + O\left(\frac{1}{\sqrt{\tau}}\right). \tag{E4}$$

From Eq. (E4), we may conclude that (E3) is only valid if $\tau > \frac{2\varepsilon^*}{N}$ and $\tau > N + 1$.

b. Case 2: Odd size N and $\varepsilon^* \neq 1$

For odd network sizes N , all eigenvalues a_k are twofold-degenerate. All eigenvalues can be computed using (E3) provided that $\varepsilon^* \neq 1$. However, special attention is required for eigenvalues a_k with indices $k = \frac{N+1}{2}$ and $k = \frac{N-1}{2}$. In that case, the eigenvalue equation (E1) becomes

$$\begin{pmatrix} -\frac{\alpha}{2}[\varepsilon^*(N + 1) + N - 1] & \frac{N+1}{2}\sqrt{\frac{N-1}{2} + \varepsilon^*\alpha^2} \\ \frac{N+1}{2}\sqrt{\frac{N-1}{2} + \varepsilon^*\alpha^2} & -\frac{\alpha}{2}[\varepsilon^*(N - 1) + N + 1] \end{pmatrix} \begin{pmatrix} \alpha_{(N-1)/2} \\ \beta_{(N-1)/2} \end{pmatrix} = \xi_{(N-1)/2}^{(1)} \begin{pmatrix} \alpha_{(N-1)/2} \\ \beta_{(N-1)/2} \end{pmatrix}$$

whose eigenvalues are distinct:

$$\xi_{(N-1)/2}^{(1)} = \frac{\alpha(N - \varepsilon^*)}{2} \pm \sqrt{\left(\frac{\alpha(N - \varepsilon^*)}{2}\right)^2 + \frac{1}{8}(N + 1)^2(N - 1)}.$$

The corresponding eigenvectors are

$$\begin{pmatrix} \alpha_{(N-1)/2} \\ \beta_{(N-1)/2} \end{pmatrix} = \begin{pmatrix} \alpha(N - \varepsilon^*) \pm \sqrt{\alpha^2(N - \varepsilon^*)^2 + (N + 1)^2\left(\frac{N-1}{2} + \varepsilon^*\alpha^2\right)} \\ (N + 1)\sqrt{\frac{N-1}{2} + \varepsilon^*\alpha^2} \end{pmatrix}.$$

We will not continue our analysis for the $O(\alpha^2)$ terms, because the computations are tedious. Our final result is

$$\alpha^2 \xi_{(N-1)/2} = -\frac{N - 1}{2} \frac{N + 1}{2} + \alpha \frac{\alpha(N - \varepsilon^*)}{2} \pm \sqrt{\left(\frac{\alpha(N - \varepsilon^*)}{2}\right)^2 + \frac{1}{8}(N + 1)^2(N - 1) + O(\alpha^2)}.$$

Using $\alpha^2 = \frac{1}{\tau}$, we find the following relationship for the eigenvalues:

$$\xi_{(N-1)/2} = -\frac{1}{4}\tau(N - 1)(N + 1) \pm \sqrt{\tau}(N + 1)\sqrt{\frac{N - 1}{2}} + O(1). \tag{E5}$$

The relation (E5) is a valid perturbation expansion if $\tau > \frac{8}{N-1}$. Since the computations of the second-order terms are tedious, we have omitted them here. The key observation is that the eigenvalue $\xi_{(N-1)/2}$ scales with an $O(\sqrt{\tau})$ term, which is not the case for even-sized networks. We have not found any physical or intuitive reasoning why this is the case.

c. Case 3: Even size N and $\varepsilon^* = 1$

In this case, we construct the M -matrix for $k \neq N/2$,

$$M = \begin{pmatrix} M_{kk} & M_{k,N-k} \\ M_{N-k,k} & M_{N-k,N-k} \end{pmatrix},$$

where

$$M_{k,N-k} = \sum_{\substack{m=1 \\ m \neq k \\ m \neq N-k}}^N \frac{W_{k,m}W_{m,N-k}}{\xi_k^{(0)} - \xi_m^{(0)}}.$$

We find

$$M_{kk} = \frac{k(N-k)(N+1)}{(2k-N-1)(2k-N+1)} + k + \alpha^2 \frac{k^2 + (N-k)^2 + N}{(2k-N-1)(2k-N+1)}.$$

In most cases, $M_{k,N-k} = 0$ because the product $W_{k,m}W_{m,N-k}$ is only nonzero for $m = k-1$ or $m = k+1$, and $m = N-k+1$ or $m = N-k-1$. Hence, the product is only non-zero if $k = \frac{N}{2} - 1$. Thus, for $k \neq \frac{N}{2} - 1$, the second-order correction of the eigenvalues is unique and the eigenvalues follow as

$$\alpha^2 \xi_k = -k(N-k) - \alpha^2 N + \alpha^2 \left(\frac{k(N-k)(N+1)}{(2k-N-1)(2k-N+1)} + k + \alpha^2 \frac{k^2 + (N-k)^2 + N}{(2k-N-1)(2k-N+1)} \right) + O(\alpha^3).$$

Using $\alpha^2 = \frac{1}{\tau}$, we find the following relationship for the eigenvalues:

$$\xi_k = -\tau k(N-k) + k - N + \frac{k(N-k)(N+1)}{(2k-N-1)(2k-N+1)} + O\left(\frac{1}{\sqrt{\tau}}\right). \quad (\text{E6})$$

For $k = \frac{N}{2} - 1$, additional work is required because the off-diagonal terms are nonzero. The M -matrix is in this case

$$M = \begin{pmatrix} \frac{1}{12}(N-2)(N^2+3N+8) & \frac{N}{2}\left(\frac{N}{2}+1\right)\sqrt{\left(\frac{N}{2}-1+\alpha^2\right)\left(\frac{N}{2}+\alpha^2\right)} \\ \frac{N}{2}\left(\frac{N}{2}+1\right)\sqrt{\left(\frac{N}{2}-1+\alpha^2\right)\left(\frac{N}{2}+\alpha^2\right)} & \frac{1}{12}(N+2)(N^2-N+4) \end{pmatrix}$$

whose eigenvalues are

$$\xi_k^{(2)} = \frac{N^3}{12} + \frac{N^2}{12} + \frac{N}{6} - \frac{1}{3} \pm \sqrt{1 + \left(\frac{N}{2}\right)^3 \left(\frac{N}{2}+1\right)^2 \left(\frac{N}{2}-1\right)}$$

thus the total eigenvalue expansion equals

$$\xi_k = -\tau \left(\frac{N}{2}-1\right) \left(\frac{N}{2}+1\right) + \frac{N^3}{12} + \frac{N^2}{12} - \frac{5N}{6} - \frac{1}{3} \pm \sqrt{1 + \left(\frac{N}{2}\right)^3 \left(\frac{N}{2}+1\right)^2 \left(\frac{N}{2}-1\right)}.$$

d. Case 4: Odd size N and $\varepsilon^* = 1$

For the case $k \neq \frac{N-1}{2}$, the eigenvalues follow from (E6) and the result for $k = \frac{N-1}{2}$ is described in (E5).

Finally introducing $\tilde{k} = k+1$, such that the index \tilde{k} runs from 1 to $N+1$, finalizes the proof.

3. Limit $\varepsilon^* \rightarrow 0$

For self-infection rates $\varepsilon^* < \frac{1}{N}$, Gershgorin's circle theorem leads to a tight bound for the smallest eigenvalue ξ_{N+1} . The case $\tau > \tau_c$ appeared earlier in Ref. [48] (Corollary 3).

Proof. We denote the (not necessarily ordered) eigenvalues ξ_1, \dots, ξ_{N+1} of the transition matrix P from Eq. (2). Given the scaled birth rate $\tilde{\lambda}_k$ and death rate $\tilde{\mu}_k$, Gershgorin's circle theorem provides the following bounds for the eigenvalues:

$$|\xi_k + \tilde{\lambda}_k + \tilde{\mu}_k| \leq \tilde{\lambda}_{k-1} + \tilde{\mu}_{k+1}.$$

Substituting the scaled birth rate $\tilde{\lambda}_k = (\tau k + 1)(N - k)$ and the scaled death rate $\tilde{\mu}_k = k$, we find

$$f(k) \leq \xi_k \leq 1 + \varepsilon^* + \tau(2k - N - 1), \quad (\text{E7})$$

where the lower bound $f(k)$ equals

$$f(k) = -\tau[(k-1)(N-k+1) + k(N-k)] - \varepsilon^*[2N - 2k + 1] - [2k + 1]. \quad (\text{E8})$$

The lower bound $f(k)$ is negative for all $k = 1, \dots, N+1$. The upper bound is most negative for $k = 1$, hence $\min_k \xi_k \leq 1 + \varepsilon^* - \tau(N-1)$. Using $\tau = x\tau_c^{(1)} = \frac{x}{N-1}$, we find $\min_k \xi_k \leq 1 - x + \varepsilon^* < 0$ above the epidemic threshold

($x > 1$). For the remaining eigenvalues ξ_k , the upper bound is larger than zero, which is not confining. Simulations also indicate that the upper bound is very loose. Instead, we focus on the lower bound $f(k)$.

a. Above the epidemic threshold

The lower bound $f(k)$ is the smallest when $\frac{df}{dk} = 0$, and we find⁸

$$\frac{df}{dk}(\hat{k}) = -\tau(2N - 4\hat{k} + 2) + 2\varepsilon^* - 2 = 0. \quad (\text{E9})$$

Solving for \hat{k} gives

$$\hat{k} = \frac{1 - \varepsilon^*}{2\tau} + \frac{N+1}{2}.$$

Since we consider the case $\varepsilon^* < \frac{1}{N}$, the effective self-infection rate ε^* can be neglected,

$$\hat{k} = \frac{1}{2\tau} + \frac{N+1}{2}. \quad (\text{E10})$$

Hence, \hat{k} is at least larger than $N/2$. The lower bound becomes

$$f(\hat{k}) = -\frac{1}{2\tau} - \frac{3}{2} - N - \frac{\tau N(N-1)}{2} + \varepsilon^* \left[\frac{1}{\tau} - N \right].$$

⁸We assume here that the function $f(k)$ is varying slowly, which means that the difference between $f(k+1)$ and $f(k)$ is small for all k . Since the function $f(k)$ is a quadratic function in k , the function $f(k)$ indeed varies sufficiently slowly.

Using the normalized effective infection rate $x = \tau(N - 1)$, we approximately find

$$f(\hat{k}) \approx -\left(\frac{1}{2x} + 1 + \frac{x}{2}\right)N + \left(\frac{1}{2x} - \frac{3}{2}\right). \quad (\text{E11})$$

The lower bound (E11) holds for all eigenvalues ξ_k where $1 \leq k \leq N + 1$. Thus we may conclude that

$$\xi_{N+1} \gtrsim -\left(\frac{1}{2x} + 1 + \frac{x}{2}\right)N.$$

b. Below the epidemic threshold

If $\tau < \tau_c^{(1)} = \frac{1}{N-1}$, the lower bound $f(k)$ is the smallest for $\hat{k} = N - 1$. We find

$$f(\hat{k}) = -\tau(3N - 5) - 2N + 1.$$

Using $\tau = \frac{x}{N-1}$ and $x < 1$, we find approximately

$$f(\hat{k}) \approx -2N + 1 - 3x. \quad (\text{E12})$$

Equation (E12) holds for all eigenvalues ξ_k , with $1 \leq k \leq N + 1$, thus we conclude that

$$\xi_{N+1} \gtrsim -2N.$$

4. The limit $\tau \rightarrow 0$

If the effective infection rate $\tau = 0$, then the ε -SIS model reduces to a birth and death process with linear rates that can be solved exactly for any time t and any number of initially infected nodes [19]. The eigenvalue ratio ρ in the limit of small effective infection rates τ is approximately $\rho = \xi_3/\xi_2 \approx 3/2$, because the second-largest eigenvalue $\xi_2 \approx -2$ and $\xi_3 \approx -3$. Thus, metastability cannot be observed for small effective infection rates τ .

5. Final considerations

Apart from limit cases and bounds, the second-largest eigenvalue ξ_2 can be computed using the following approach.

Theorem E.2 (Van Doorn *et al.* [35]). The convergence rate $-\xi_2$ equals

$$\max_{\mathbf{d} > \mathbf{0}} \min_{1 \leq k \leq N} \alpha_k = -\xi_2 = \min_{\mathbf{d} > \mathbf{0}} \max_{1 \leq k \leq N} \alpha_k, \quad (\text{E13})$$

where $\mathbf{d} = (d_1, \dots, d_N)$, and $d_i > 0$ for $i = 1, \dots, N$ and

$$\begin{aligned} \alpha_k = \tau & \left[\left(\frac{d_{k+1}}{d_k} - 1 \right) k^2 + \left(1 - \frac{d_{k+1}}{d_k} \right) kN + 2k - N - 1 \right] \\ & + \varepsilon^* \left[\left(\frac{d_{k+1}}{d_k} - 1 \right) k + \left(1 - \frac{d_{k+1}}{d_k} \right) N + 1 \right] \\ & + \left[\left(1 - \frac{d_{k-1}}{d_k} \right) k + \frac{d_{k-1}}{d_k} \right] \end{aligned}$$

for $k = 1, \dots, N$ and $d_0 = d_{N+1} = 0$.

Theorem E.2 associates the computation of the second-largest eigenvalue ξ_2 of the transition matrix P to the finding of a suitable, positive vector \mathbf{d} . Equation (E13) illustrates that choosing any positive vector \mathbf{d} directly provides lower and upper bounds for the convergence rate ξ_2 . Unfortunately, simply generating random values for the vector \mathbf{d} does not provide sharp bounds for the second-largest eigenvalue ξ_2 .

As an example, we consider $\mathbf{d} = \mathbf{u}$, where \mathbf{u} is the $N \times 1$ all-ones vector. According to Theorem E.2, the convergence rate ξ_2 is then bounded by

$$-\tau(N - 1) + 1 + \varepsilon^* \leq -\xi_2 \leq \tau(N - 1) + 1 + \varepsilon^*. \quad (\text{E14})$$

If the effective infection rate τ is larger than the mean-field epidemic threshold $\tau_c^{(1)} = \frac{1}{N-1}$, the lower bound in (E14) is negative and therefore not confining. For $\tau < \tau_c$, the lower bound in (E14) appears to be a loose bound. In the limit $\tau \rightarrow 0$, the convergence rate equals $-\xi_2 = 1 + \varepsilon^*$, which agrees with Theorem V.1. The upper bound is positive in both cases, and is at least 1, but it appears to be a loose bound as well.

[1] P. Cirillo and N. Taleb, Tail risk of contagious diseases, *Nat. Phys.* **16**, 606 (2020).
 [2] W. Dhouib, J. Maatoug, I. Ayouni, N. Zammit, R. Ghammem, S. Ben Fredj, and H. Ghannem, The incubation period during the pandemic of COVID-19: A systematic review and meta-analysis, *Syst. Rev.* **10**, 101 (2021).
 [3] W. v. d. Toorn, D. Oh, D. Bourquain, J. Michel, E. Krause, A. Nitsche, and M. v. Kleist, An intra-host SARS-CoV-2 dynamics model to assess testing and quarantine strategies for incoming travelers, contact management, and de-isolation, *Patterns* **2**, 100262 (2021).
 [4] P. Van Mieghem and Q. Liu, Explicit non-Markovian susceptible-infected-susceptible mean-field epidemic threshold for Weibull and Gamma infections but Poisson curings, *Phys. Rev. E* **100**, 022317 (2019).
 [5] R. Pastor-Satorras, C. Castellano, P. Van Mieghem, and A. Vespignani, Epidemic processes in complex networks, *Rev. Mod. Phys.* **87**, 925 (2015).
 [6] I. Nåsell, *Extinction and Quasi-Stationarity in the Stochastic Logistic SIS Model*, 1st ed. (Springer-Verlag, Berlin, 2011)
 [7] P. Van Mieghem, Explosive phase transition in susceptible-infected-susceptible epidemics with arbitrary small but nonzero self-infection rate, *Phys. Rev. E* **101**, 032303 (2020).
 [8] J. A. Jacquez and C. P. Simon, The stochastic SI model with recruitment and deaths I. comparison with the closed SIS model, *Math. Biosci.* **117**, 77 (1993).
 [9] E. Cator and P. Van Mieghem, Susceptible-infected-susceptible epidemics on the complete graph and the star graph: Exact analysis, *Phys. Rev. E* **87**, 012811 (2013).
 [10] M. M. de Oliveira and R. Dickman, How to simulate the quasi-stationary state, *Phys. Rev. E* **71**, 016129 (2005).
 [11] M. Keeling and J. Ross, On methods for studying stochastic disease dynamics, *J. R. Soc. Interface* **5**, 171 (2008).
 [12] A. L. Hill, D. G. Rand, M. A. Nowak, and N. A. Christakis, Emotions as infectious diseases in a large social network: the SISa model, *Proc. R. Soc. B* **277**, 3827 (2010).

- [13] P. Van Mieghem and E. Cator, Epidemics in networks with nodal self-infection and the epidemic threshold, *Phys. Rev. E* **86**, 016116 (2012).
- [14] P. Simon, M. Taylor, and I. Kiss, Exact epidemic models on graphs using graph-automorphism driven lumping, *J. Math. Biol.* **62**, 479 (2011).
- [15] A. Lajmanovich and J. A. Yorke, A deterministic model for gonorrhea in a nonhomogeneous population, *Math. Biosci.* **28**, 221 (1976).
- [16] P. Van Mieghem, The N-intertwined SIS epidemic network model, *Computing* **93**, 147 (2011).
- [17] K. Devriendt and P. Van Mieghem, Unified mean-field framework for susceptible-infected-susceptible epidemics on networks, based on graph partitioning and the isoperimetric inequality, *Phys. Rev. E* **96**, 052314 (2017).
- [18] P. Van Mieghem and R. van de Bovenkamp, Accuracy criterion for the mean-field approximation in susceptible-infected-susceptible epidemics on networks, *Phys. Rev. E* **91**, 032812 (2015).
- [19] D. G. Kendall, On the Generalized “Birth-and-Death” Process, *Ann. Math. Stat.* **19**, 1 (1948).
- [20] M. Assaf and B. Meerson, Spectral Theory of Metastability and Extinction in Birth-Death Systems, *Phys. Rev. Lett.* **97**, 200602 (2006).
- [21] P. Van Mieghem and F. Wang, Time dependence of susceptible-infected-susceptible epidemics on networks with nodal self-infections, *Phys. Rev. E* **101**, 052310 (2020).
- [22] S. Karlin and J. McGregor, Coincidence probabilities, *Pac. J. Math.* **9**, 1141 (1959).
- [23] P. Van Mieghem, *Graph Spectra for Complex Networks*, 1st ed. (Cambridge University Press, Cambridge, 2011).
- [24] C. R. Doering, K. V. Sargsyan, and L. M. Sander, Extinction times for birth-death processes: Exact results, continuum asymptotics, and the failure of the Fokker-Planck approximation, *Multiscale Model. Simul.* **3**, 283 (2005).
- [25] J. R. Artalejo, On the time to extinction from quasi-stationarity: A unified approach, *Physica A* **391**, 4483 (2012).
- [26] P. Holme and L. Tupikina, Epidemic extinction in networks: insights from the 12 110 smallest graphs, *New J. Phys.* **20**, 113042 (2018).
- [27] P. Van Mieghem, Decay towards the overall-healthy state in SIS epidemics on networks, [arXiv:1310.3980](https://arxiv.org/abs/1310.3980) [math.PR].
- [28] R. van de Bovenkamp and P. Van Mieghem, Survival time of the susceptible-infected-susceptible infection process on a graph, *Phys. Rev. E* **92**, 032806 (2015).
- [29] H. Andersson and B. Djehiche, A threshold limit theorem for the stochastic logistic epidemic, *J. Appl. Probab.* **35**, 662 (1998).
- [30] R. v. d. Bovenkamp and P. Van Mieghem, Time to Metastable State in SIS Epidemics on Graphs, in *2014 Tenth International Conference on Signal-Image Technology & Internet-Based Systems (SITIS)* (IEEE Computer Society, Los Alamitos, CA, 2014), pp. 347–354.
- [31] Z. He and P. Van Mieghem, The spreading time in SIS epidemics on networks, *Physica A* **494**, 317 (2018).
- [32] P. Van Mieghem, *Performance Analysis of Complex Networks and Systems* (Cambridge University Press, Cambridge, UK, 2014).
- [33] B. N. Parlett, *The Symmetric Eigenvalue Problem*, 1st ed. Classics in Applied Mathematics (Society for Industrial and Applied Mathematics, Philadelphia, PA, 1980).
- [34] A. Ganesh, L. Massoulié, and D. Towsley, The effect of network topology on the spread of epidemics, in *Proceedings IEEE 24th Annual Joint Conference of the IEEE Computer and Communications Societies* (IEEE, Piscataway, NJ, 2005), Vol. 2, pp. 1455–1466.
- [35] E. A. van Doorn, A. I. Zeifman, and T. L. Panfilova, Bounds and asymptotics for the rate of convergence of birth-death processes, *Theory Probab. Appl.* **54**, 97 (2010).
- [36] B. Prasse, K. Devriendt, and P. Van Mieghem, Clustering for epidemics on networks: A geometric approach, *Chaos* **31**, 063115 (2021).
- [37] Y. Wang, D. Chakrabarti, C. Wang, and C. Faloutsos, Epidemic spreading in real networks: An eigenvalue viewpoint, in *Proceedings of the 22nd International Symposium on Reliable Distributed Systems* (IEEE, Piscataway, NJ, 2003).
- [38] P. L. Simon and I. Z. Kiss, From exact stochastic to mean-field ODE models: a new approach to prove convergence results, *IMA J. Appl. Math.* **78**, 945 (2013).
- [39] P. Van Mieghem and R. van de Bovenkamp, Non-Markovian Infection Spread Dramatically Alters the Susceptible-Infected-Susceptible Epidemic Threshold in Networks, *Phys. Rev. Lett.* **110**, 108701 (2013).
- [40] D. Guo, S. Trajanovski, R. van de Bovenkamp, H. Wang, and P. Van Mieghem, Epidemic threshold and topological structure of susceptible-infectious-susceptible epidemics in adaptive networks, *Phys. Rev. E* **88**, 042802 (2013).
- [41] G. H. Golub and C. F. Van Loan, *Matrix Computations*, 3rd ed. (The Johns Hopkins University Press, Baltimore, 1996).
- [42] E. Cator and P. Van Mieghem, Nodal infection in Markovian susceptible-infected-susceptible and susceptible-infected-removed epidemics on networks are non-negatively correlated, *Phys. Rev. E* **89**, 052802 (2014).
- [43] B. Prasse and P. Van Mieghem, Time-dependent solution of the NIMFA equations around the epidemic threshold, *J. Math. Biol.* **81**, 1299 (2020).
- [44] M. Abramowitz and I. A. Stegun, *Handbook of Mathematical Functions: With Formulas, Graphs, and Mathematical Tables*, 9th ed. (Dover Publications, New York, 1965), Vol. 55.
- [45] D. J. Griffiths and D. F. Schroeter, *Introduction to Quantum Mechanics*, 3rd ed. (Cambridge University Press, Cambridge, 2018).
- [46] J. J. Sakurai and J. Napolitano, *Modern Quantum Mechanics*, 2nd ed. (Addison-Wesley, Boston, 2011).
- [47] M. A. Achterberg and P. Van Mieghem, Exact solution of heterogeneous Markovian SI epidemics on networks (unpublished).
- [48] P. Van Mieghem, J. Omic, and R. Kooij, Virus spread in networks, *IEEE/ACM Trans. Networking* **17**, 1 (2009).